Bioscience Reports (2018) **38** BSR20180527
https://doi.org/10.1042/BSR20180527

Research Article

Controlling the regioselectivity and stereospecificity of FAD-dependent polyamine oxidases with the use of amine-attached guide molecules as conformational modulators

Tuomo A. Keinänen[1], Nikolay Grigorenko[3], Alex R. Khomutov[4], Qingqiu Huang[2], Anne Uimari[5], Leena Alhonen[1], Mervi T. Hyvönen[1] and Jouko Vepsäläinen[1]

[1]School of Pharmacy, Biocenter Kuopio, University of Eastern Finland, Kuopio Campus, P.O. Box 1627, Kuopio FI-70211, Finland; [2]MacCHESS at the Cornell High Energy Synchrotron Source, Cornell University Ithaca, NY 14853-8001, U.S.A.; [3]BASF Schweiz AG, Dispersions and Pigments Division, Klybeckstrasse 141, P.O. Box CH 4002, Basel, Switzerland; [4]Engelhardt Institute of Molecular Biology, Russian Academy of Sciences, Vavilov St 32, Moscow 119991, Russia; [5]Natural Resources Institute Finland, Natural Resources Division, Neulaniementie 5, Kuopio FI-70210, Finland

Correspondence: Tuomo A. Keinänen (tuomo.keinanen@uef.fi)

Enzymes generally display strict stereospecificity and regioselectivity for their substrates. Here by using FAD-dependent human acetylpolyamine oxidase (APAO), human spermine (Spm) oxidase (SMOX) and yeast polyamine oxidase (Fms1), we demonstrate that these fundamental properties of the enzymes may be regulated using simple guide molecules, being either covalently attached to polyamines or used as a supplement to the substrate mixtures. APAO, which naturally metabolizes achiral N^1-acetylated polyamines, displays aldehyde-controllable stereospecificity with chiral 1-methylated polyamines, like *(R)*- and *(S)*-1-methylspermidine (1,8-diamino-5-azanonane) (1-MeSpd). Among the novel N^1-acyl derivatives of MeSpd, isonicotinic acid (P4) or benzoic acid (Bz) with *(R)*-MeSpd had K_m of 3.6 ± 0.6/1.2 ± 0.7 μM and k_{cat} of 5.2 ± 0.6/4.6 ± 0.7 s^{-1} respectively, while N^1-AcSpd had K_m 8.2 ± 0.4 μM and k_{cat} 2.7 ± 0.0 s^{-1}. On the contrary, corresponding *(S)*-MeSpd amides were practically inactive (k_{cat} < 0.03 s^{-1}) but they retained micromole level K_m for APAO. SMOX did not metabolize any of the tested compounds (k_{cat} < 0.05 s^{-1}) that acted as non-competitive inhibitors having $K_i \geq 155$ μM for SMOX. In addition, we tested *(R,R)*-1,12-bis-methylspermine (2,13-diamino-5,10-diazatetradecane) *(R,R)*-(Me_2Spm) and *(S,S)*-Me_2Spm as substrates for Fms1. Fms1 preferred *(S,S)*- to *(R,R)*-diastereoisomer, but with notably lower k_{cat} in comparison with spermine. Interestingly, Fms1 was prone to aldehyde supplementation in its regioselectivity, i.e. the cleavage site of spermidine. Thus, aldehyde supplementation to generate aldimines or *N*-terminal substituents in polyamines, i.e. attachment of guide molecule, generates novel ligands with altered charge distribution changing the binding and catalytic properties with polyamine oxidases. This provides means for exploiting hidden capabilities of polyamine oxidases for controlling their regioselectivity and stereospecificity.

Received: 25 March 2018
Revised: 03 July 2018
Accepted: 05 July 2018

Accepted Manuscript Online: 13 July 2018
Version of Record published: 29 August 2018

Introduction

The polyamines spermidine (Spd) and spermine (Spm) and their diamine precursor putrescine (Put) are essential cellular constituents in eukaryotic organisms [1] (Figure 1A). Their intracellular levels are strictly

Bioscience Reports (2018) **38** BSR20180527
https://doi.org/10.1042/BSR20180527

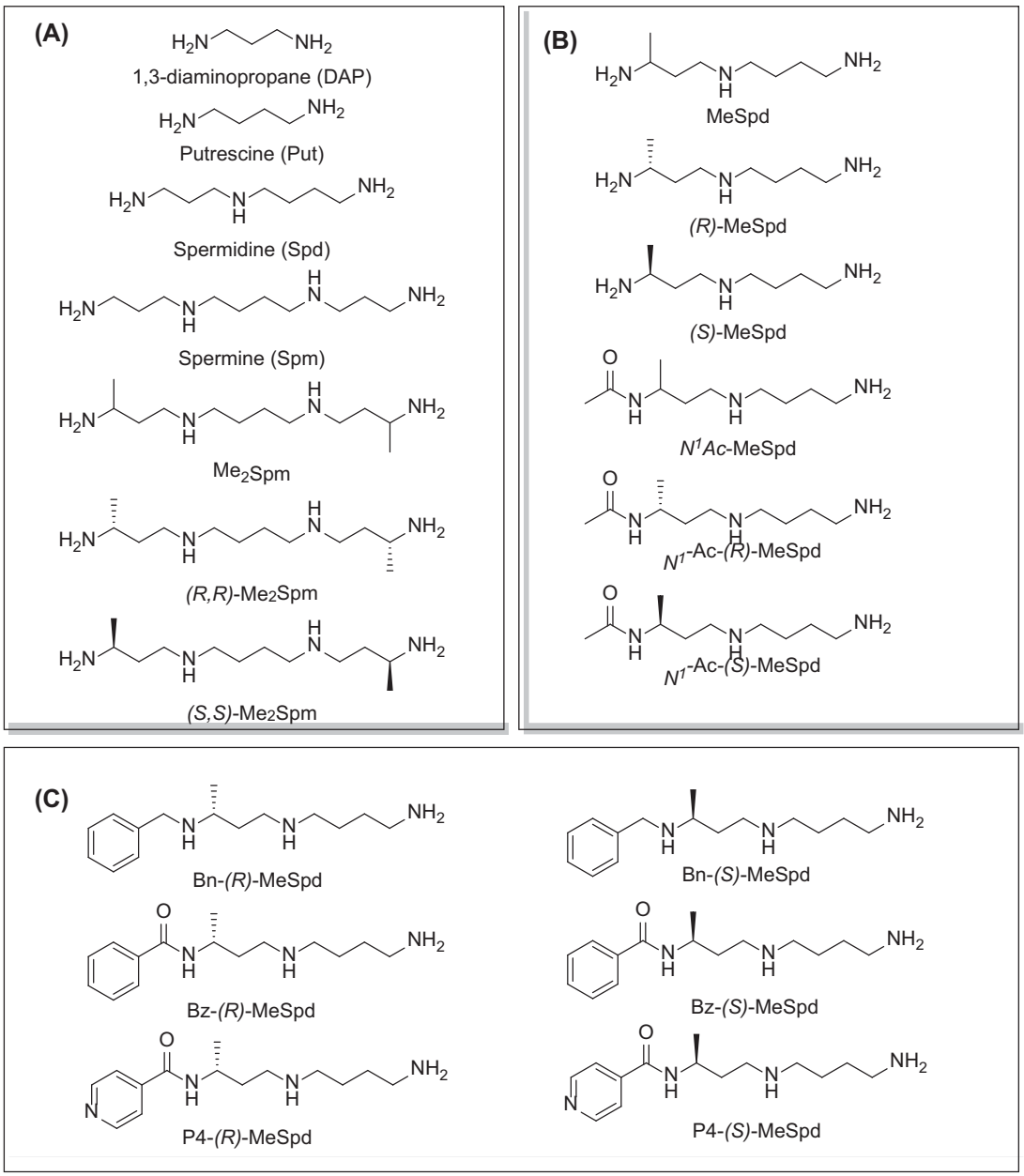

Figure 1. Chemical structures of the reference and tested compounds

Structures of (**A**) 1,3-Diaminopropane (DAP), natural polyamines and dimethylated analogues of Spm. (**B**) 1-Methylated spermidine analogues and their N^1-acetylated derivatives. (**C**) Guide molecule-derivatives of *(R)*-MeSpd and *(S)*-MeSpd. Abbreviation: MeSpd, 1-methylspermidine (1,8-diamino-5-azanonane).

regulated by *de novo* synthesis, active transport, excretion and catabolism by a complex cellular regulatory network [2,3]. Interconversion of Spm into Spd is enzymatically regulated by FAD-dependent spermine oxidase (SMOX; EC 1.5.3.16) or by consequent actions of Spd/Spm-N^1-acetyltransferase (SSAT; EC 2.3.1.57) and acetylpolyamine oxidase (APAO; EC 1.5.3.13) [4,5]. Recent studies clearly show that polyamine metabolism is disturbed in a variety of diseases or medical disorders, such as cancer, brain insult and diabetes [6,7]. Furthermore, polyamine metabolism differs between parasites, microbes and the host, which could be used for developing novel therapies [8].

Oxidative catabolism of polyamines generates acrolein and reactive oxygen species (ROS) like hydrogen peroxide, which in excess are harmful to cells. Dysregulation of SMOX and activated Spm catabolism are associated with

inflammation-mediated development of cancer [9]. There is direct evidence that the induction of SMOX during neoplastic transformation leads to the development of colon and gastric cancer. Furthermore, in cancer cells APAO has been shown to detoxify *N*-alkylated polyamine analogues [10], while induction of SMOX is responsible for the toxic effects of *N*-alkylated polyamine analogues [11]. Thus, APAO and SMOX sometimes play opposite roles in determining drug sensitivity of cancer cells. So far, determinations of crystal structure of native APAO and SMOX have been unsuccessful, although recently several crystal structures of slightly mutated murine APAO were reported [12]. The latter data in combination with the available yeast polyamine oxidase (Fms1) and maize PAO crystal structures, computer modelling and experiments with targeted point mutations into recombinant proteins have been used to study the possible structure-activity determinants of APAO and SMOX [13-16]. All the previous enzymes are available as recombinant proteins and their structure-activity properties *in vitro* have been relatively well characterized. Unfortunately, obtaining highly selective small-molecule inhibition of either APAO or SMOX has been unsuccessful, leaving gene silencing as the only viable option to investigate the physiological functions of these enzymes [17].

α-Methylation is an efficient chemical modification to protect amine-based drugs against degradation by cellular mono- and diamine oxidases and to modulate drug ADME properties [18,19]. Some of the α-methylated drug derivatives have proved to be efficient inhibitors of parent oxidases that catabolize biogenic amines [18]. Racemic α-methylated polyamines 1-methylspermidine (1,8-diamino-5-azanonane) (MeSpd), MeSpm and 1,12-bis-methylspermine (2,13-diamino-5,10-diazatetradecane) (Me_2Spm) were synthesized by Lakanen et al. [20] (Figure 1A/B). They were shown to be metabolically stable, i.e. not acetylated by SSAT with the exception of MeSpm, and were able to substitute natural polyamines in supporting cell growth under natural polyamine deprivation [20,21]. MeSpd and Me_2Spm are not so readily metabolized *in vivo* as Spd and Spm, and *in vitro* they are not catabolized to toxic compounds by serum amine oxidases [20,22]. Thus, they seem to be ideal candidates for *in vivo* use [23,24]. Although natural polyamines are achiral, we have discovered the hidden stereospecificity of APAO, SMOX and deoxyhypusine synthase (DHS; 2.5.1.46) [24-26]. APAO preferably oxidizes the *(R)*-enantiomer of N^1-Ac-MeSpd [24]. *(S,S)*-Me_2Spm is a substrate of SMOX while *(R,R)*-Me_2Spm is not metabolized by the enzyme [25], and *(S)*-MeSpd is a source of aminobutyl fragment in DHS reaction [26]. Furthermore, we have recently shown that polyamine transport system and the key enzymes of polyamine metabolism, namely ornithine decarboxylase (ODC), *S*-adenosyl-*L*-methionine decarboxylase (AdoMetDC) and SSAT are divergently regulated by chiral *C*-methylated polyamine analogues [27,28]. Our earlier findings indicate that the stereospecificity of FAD-dependent human APAO can be altered with the aid of simple guide molecules [29]. Guide effects of aromatic aldehydes in APAO reaction using racemic MeSpd as a substrate were very clear and unexpected. Benzaldehyde stimulated the splitting of *(R)*-MeSpd, pyridoxal—splitting of *(S)*-MeSpd, while 4-pyridinealdehyde was not able to induce stereospecificity [29]. All above prompted us to synthetize a set of earlier unknown N^1-benzylated (Bn) or N^1-acylated, i.e. isonicotinic acid (P4) and benzoic acid (Bz) amide derivatives of *(R)*- and *(S)*-MeSpd to further explore characteristics of FAD-dependent amino oxidoreductases (Figure 1C).

Here we studied the substrate specificities of SMOX and APAO for N^1-alkylated or N^1-acylated derivatives of *(R)*- and *(S)*-MeSpd and the effects of supplemented aldehydes on Fms1, that readily catalyses the oxidation of N^1-acetylated Spd and Spm. We also used *(R,R)*-Me_2Spm and *(S,S)*-Me_2Spm to gain insight into how 1,12-bis-methylation of Spm and configuration of chiral centres affects the substrate properties and binding to the active centre of Fms1 (Figure 1A). N^1-Acetylated derivatives of 1-MeSpd were synthesized to complete the series of analogues, tested with the Fms1 and to compare the results with the known stereospecificity of APAO (Figure 1B). Obtained data demonstrate for the first time that stereospecificity and regiospecificity of FAD-dependent polyamine oxidases could be controlled with the conformationally restricted ligands exploiting existing conformational landscapes in enzyme without protein engineering.

Experimental procedures

Materials

All the commercially available chemicals were purchased from Sigma–Aldrich. *(R,R)*-Me_2Spm, *(S,S)*-Me_2Spm and racemic Me_2Spm, *(R)*-MeSpd and *(S)*-MeSpd enantiomers and their covalently modified guide molecule derivatives were synthesized essentially as described in [24].

Production of recombinant enzymes and enzyme tests

The production of human recombinant APAO, SMOX and yeast Fms1 has been described earlier [16,22]. Substrate and aldehyde supplement concentrations and experimental conditions are described in Figures and Tables captions. HPLC with post-column *o*-phthalaldehyde-derivatization was used to determine the concentrations of the reaction

Bioscience Reports (2018) **38** BSR20180527
https://doi.org/10.1042/BSR20180527

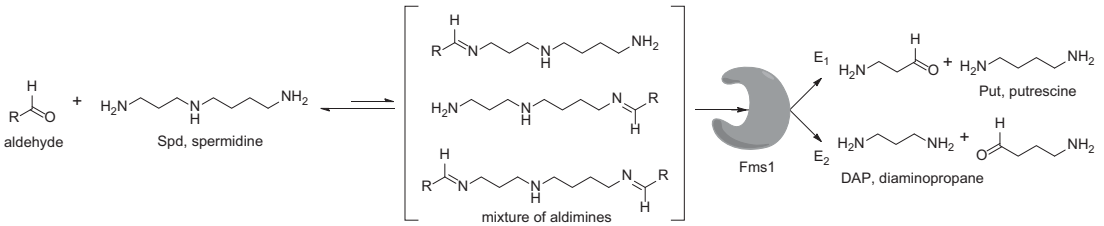

Figure 2. Simplified sketch showing chemical principle for using aldehyde supplementation to generate *in situ* aldimines mimicking the charges of *N*-acetylated Spd species

In aqueous solution, equilibrium is strongly favouring free Spd and aldehyde species. However, by increasing aldehyde concentration it is possible to increase aldimine pool concentration, e.g. Table 4 and accelerate Fms1-mediated degradation of Spd pool.

products Put and 1,3-diaminopropane (DAP) or butane-1,3-diamine respectively as described in [30]. Fms1 activity was determined essentially as described for human recombinant APAO, but reactions were carried out in 100 mM Glycine-NaOH buffer at pH 9.0 in a water bath at +25°C [29,30]. Reactions for kinetic value determinations were carried out at pH 9.0 in 100 mM Glycine-NaOH in triplicates by using 25, 50, 75, 100, 200, 400 and 600 μM substrate concentrations for Spm and for Me_2Spm but 600 μM concentration was replaced with 1 mM concentration in Me_2Spm series. Kinetic values were determined by using Michaelis–Menten equation and non-linear regression by using GraphPad Prism software 5.03 with enzyme kinetic template. Fms1 activity compared with pH was determined by using 1 mM Spm with 0.1 μg of Fms1 in 170 mM Bis/Tris buffer at pH 7.4, 8.0, 8.25, 8.5, 8.75, 9.0, 9.25 and 9.5 incubated 4 min at 25°C. k_{cat} values were determined using an M_r of 55382 for human recombinant APAO, M_r 62000 for SMOX and for Fms1 using M_r of 58833 [31].

K_i values for covalently modified MeSpd derivatives for SMOX were determined as triplicates using at least four inhibitor concentrations (25, 100, 200, 250, 500, 1000 or 2000 μM) in the presence of 25, 50 or 100 μM Spm. Reaction mixtures contained 40 units/ml horseradish peroxidase (Roche), 1 mM homovanillic acid in 100 mM Glycine-NaOH at pH 9.0 supplemented with 40 ng of SMOX. The reaction kinetics were monitored at 37°C using excitation at 315 nm and emission at 420 nm using Envision spectrofluorometer (PerkinElmer). Dilutions of fresh H_2O_2 were used as standard. GraphPad Prism 5.03 software using non-competitive non-linear Michaelis–Menten fitting was used to determine K_i values.

Preparation of rat liver extract

A Wistar rat liver was frozen in liquid nitrogen. The liver was homogenized (1+3 w/v) with Teflon potter in buffer containing 25 mM Tris/HCl pH 7.4, 1 mM DTT and 0.1 mM EDTA. Resulting homogenate was centrifuged at 12000×***g*** for 30 min at +4°C. Supernatant was divided into two portions and treated as follows: (A) incubated for 5 min at +37°C in a water bath, (B) supplemented with 20 μM MDL 72527 and incubated for 5 min at +37°C in a water bath to inactivate APAO and SMOX. A 20-μl aliquot of supernatant A or B was added in 100 mM Glycine-NaOH pH 9.5, 5 mM DTT with or without 100 μM of studied drug in a total volume of 180 μl. After 10-min incubation at +37°C, 20 μl of 50% sulphosalicylic acid (SSA) containing 100 μM diaminoheptane (DAH) was added to the reaction mixture. The samples were assayed with HPLC as described in [30].

Results and discussion

N-acylated and *N*-alkylated derivatives of *(R)*- and *(S)*-MeSpd as substrates of human recombinant APAO

N^1-acetylated derivatives of Spd and Spm are natural substrates of APAO and it has been shown that in the presence of aromatic aldehydes APAO efficiently metabolizes non-acetylated Spm and Spd. We have shown that the stimulatory effect of aldehydes on the APAO-catalysed oxidation of the polyamines is based on the *in situ* formation of comparatively unstable Schiff base between the primary amino group of the polyamine and the aldehyde, i.e. an aldimine mimicking the charge distribution of *N*-acetylated polyamines (Figure 2) [29,32]. Here we synthesized a set of novel chemically stable analogues of N^1-AcSpd mimicking *in situ* formed Schiff base derivatives of 1-MeSpd enantiomers (Figure 1C) and tested them as substrates of APAO. As shown in Table 1, the *(R)*-enantiomers of these derivatives served as excellent substrates for recombinant human APAO. P4-*(R)*-MeSpd and Bz-*(R)*-MeSpd displayed enhanced catalytic velocity over the natural substrate N^1-AcSpd. Interestingly, the respective *(S)*-enantiomers, P4-*(S)*-MeSpd

Table 1 Kinetic values of guide molecule-containing derivatives of MeSpds' with human recombinant APAO

Polyamine	K_m (μM)	V_{max} (μmol/min/mg)	k_{cat} (s^{-1})	k_{cat}/K_m (M^{-1} s^{-1})
N^1-AcSpd[1]	8.2 ± 0.4	2.97 ± 0.02	2.7 ± 0.0	(330 ± 16) × 10^3
Bz-*(R)*-MeSpd[2]	1.2 ± 0.7	5.02 ± 0.74	4.6 ± 0.7	(3800 ± 230) × 10^3
Bz-*(S)*-MeSpd[2]	0.2 ± 0.2	0.03 ± 0.00	0.03 ± 0.00	(150 ± 150) × 10^3
P4-*(R)*-MeSpd[3]	3.6 ± 0.6	5.59 ± 0.60	5.2 ± 0.6	(1400 ± 300) × 10^3
P4-*(S)*-MeSpd[3]	0.8 ± 0.2	0.02 ± 0.00	0.01 ± 0.00	(18 ± 3.1) × 10^3
Bn-*(R)*-MeSpd[4]	2.0 ± 0.1	0.15 ± 0.00	0.14 ± 0.00	(71 ± 3.5) × 10^3
Bn-*(S)*-MeSpd[4]	1.6 ± 0.6	0.03 ± 0.00	0.03 ± 0.00	(18 ± 7.1) × 10^3

Reactions were carried out three times in duplicates in 100 mM Glycine-NaOH at pH 9.5 supplemented with 5 mM DTT. Kinetic values were determined using GraphPad Prism 4.03 software using Michaelis–Menten equation with non-linear fitting (Supplementary Material 2). k_{cat} values were determined using an M_r of 55.382 for human recombinant APAO.
[1]10, 25, 50, 75, 100, 200 μM concentrations were used.
[2]2.5, 5, 7.5, 10, 25 μM concentrations were used.
[3]2.5, 5, 7.5, 10, 25, 100 μM concentrations were were used.
[4]5.0, 7.5, 10, and 25 μM concentrations were used.

Table 2 Degradation of N^1-AcSpd and *(R)*- and *(S)*-enantiomers of N^1-substituted MeSpd in rat liver supernatant

Sample	Formation of polyamine *(pmol/mg protein)*		
	Put	Spd	Spm
0 min	ND	3024 ± 89	2875 ± 94
10 min	ND	2964 ± 36	2793 ± 34
N^1-AcSpd 0 min	ND	3594 ± 18	3172 ± 30
N^1-AcSpd 10 min	4175 ± 278	3480 ± 12	3049 ± 23
N^1-AcSpd + MDL72527 10 min	ND	3436 ± 42	2984 ± 27
Bz-*(R)*-MeSpd 10 min*	5585 ± 288	2988 ± 2	3024 ± 18
P4-*(R)*-MeSpd 10 min*	8882 ± 66	2737 ± 78	3004 ± 74
Bn-*(R)*-MeSpd 10 min*	637 ± 13	3031 ± 72	2880 ± 234

Compounds were tested at 100 μM, which equalled 23000 pmol of the compound/mg of protein in the beginning of the reaction. Data are average of three individual reaction mixtures ± S.D. No detectable degradation of any of the tested compounds was found in the presence of MDL72527 (preincubation for 5 min before addition of the compound). Protein content of obtained liver homogenate was 39.2 μg/μl. Abbreviation: ND, not detectable.
**(S)*-enantiomer derivatives were not degraded by rat liver homogenate under the experimental conditions used.

and Bz-*(S)*-MeSpd, retained low K_m for APAO but practically lost their substrate properties, which renders them efficient competitive inhibitors. Amide derivatives P4-*(R)*-MeSpd and Bz-*(R)*-MeSpd were catalytically superior to Bn-*(R)*-MeSpd. Both Bn-*(R)*-MeSpd and Bn-*(S)*-MeSpd retained good affinity for APAO and the (*R*)-enantiomer displayed only five-fold higher k_{cat} than the *(S)*-enantiomer.

We and others have shown earlier that the resistance of racemic 1-MeSpd for APAO-mediated degradation is due to the fact that SSAT is incapable of N^1-acetylating it [20,24]. This was confirmed by using chemically synthesized N^1-Ac-*(R)*-MeSpd (K_m = 95 μM, k_{cat} = 9 s^{-1}) and *N*-Ac-*(S)*-MeSpd (K_m = 170 μM, k_{cat} = 1.2 s^{-1})—the former *(R)*-enantiomer is preferably metabolized by APAO [24]. Comparisons of their specificity constants, i.e. k_{cat}/K_m of *N*-Ac-*(R)*-MeSpd (94737 M^{-1} s^{-1}) and *N*-Ac-*(S)*-MeSpd (7059 M^{-1} s^{-1}) for APAO with P4-*(R)*-MeSpd and P4-*(S)*-MeSpd having bulkier substituents show that the specificity constant ratio of N^1-Ac-*(R)*-MeSpd/N^1-Ac-*(S)*-MeSpd is only 13 in comparison with 116 with P4-*(R)*-MeSpd/P4-*(S)*-MeSpd derivatives. This explains why Schiff base formed by bulky aldehydes, like pyridoxal and benzaldehyde, allows almost complete catalytic activation of either (*S*)- or *(R)*-MeSpd respectively [29]. Surprisingly, the specificity constant ratio with Bn-*(R)*-MeSpd and Bn-*(S)*-MeSpd was only four in comparison with earlier determined eight for benzaldehyde Schiff base derivatives of *(R)*-MeSpd and *(S)*-MeSpd for APAO (Table 1) [29]. Importantly, among the amide derivatives, i.e. P4-MeSpd and Bz-MeSpd, we found only (*R*)-enantiomer-activating guide molecules showing specificity constant ratios of 116 and 25 respectively (Tables 1 and 2). Our present data show that in the case of MeSpd it is possible to regulate the substrate properties of APAO by changing the stereoconfiguration of chiral centre in combination with the structure of an attached *N*-acyl/*N*-alkyl substituent. These features could be exploited in drug design by generating *N*-alkylated polyamine analogues that are resistant against APAO/SMOX-mediated degradation. Furthermore, specific inhibitors or substrates for enzymatic assays for APAO could be prepared accordingly.

Bioscience Reports (2018) **38** BSR20180527
https://doi.org/10.1042/BSR20180527

N-alkylated and amide derivatives of *(R)*- and *(S)*-MeSpd as substrates of human recombinant SMOX

SMOX was cloned in 2001 [5,33] and was soon shown to be a distinct enzyme from the earlier characterized APAO [34]. SMOX has several splice variants among which at least two are catalytically active, one being cytosolic and the other showing cytosolic/nuclear localization [35,36]. Interestingly, many *N*-alkylated polyamine analogues induce SMOX, and induction of SMOX has been attributed to analogue-mediated growth inhibition and cytotoxicity [11]. Moreover, recent data clearly show that SMOX induction is associated with the development of gastric, prostate and colon cancers [37-39]. Thus, developing specific inhibitors of SMOX is of crucial importance [40]. In addition, the use of specific substrates for SMOX and APAO would enable distinguishing between APAO and SMOX enzyme activities *in vivo*. All the tested amide analogues had K_m over 100 μM and k_{cat} below 0.05 s^{-1}. The K_i values for SMOX were 589 ± 58 μM for Bz-*(R)*-MeSpd, 846 ± 82 μM for Bz-*(S)*-MeSpd, 1277 ± 111 μM for P4-*(R)*-MeSpd and 1016 ± 79 μM for P4-*(S)*-MeSpd. Bn-*(S)*-MeSpd had K_i of 155 ± 13 μM and Bn-*(R)*-MeSpd K_i of 441 ± 32 μM, thus not being substrates of SMOX. The data on the interaction of acyl derivatives of *(R)*- and *(S)*-MeSpd, i.e. (Bz) and (P4) derivatives as well as alkyl (Bn) derivatives of MeSpd with APAO in comparison with SMOX clearly demonstrate that the tested compounds were differently recognized by these polyamine oxidases.

N-alkylated and amide derivatives of *(R)*- and *(S)*-MeSpd as substrates of amine oxidases in rat liver homogenates

Hölttä [32] originally purified APAO from the rat liver which is a good source for the enzyme. There are not much data available about the tissue distribution of APAO and SMOX in animals or humans, but the available data show that liver has the second highest APAO activity among the 13 studied organs in rat [34,41,42]. APAO prefers the N^1-Ac-*(R)*-MeSpd over to respective *(S)*-enantiomer [24]. The similar strong *(R)*-preference was true with bulky P4-, Bz- and Bn-MeSpd when rat liver supernatant was used as an enzyme source (Table 2). All the corresponding *(S)*-enantiomer derivatives were not degraded under the same experimental conditions. Complete inhibition of analogue degradation in the presence of MDL72527, an irreversible inhibitor of APAO and SMOX, clearly suggest that their degradation is mediated by APAO and/or SMOX. More importantly, human recombinant SMOX displayed very low k_{cat} and high K_i for the studied Spd derivatives (see above paragraph), thus clearly pointing to APAO as the degrading enzyme. These data indicate that *(S)*-1-methylation renders Spd analogue derivatives stable and could therefore be used to stabilize previously developed *N*-alkylated polyamine analogues for *in vivo* use. Furthermore, introduction of 1-methyl group could also alter biological response in comparison with parent compound [19,43].

Substrate properties of Fms1 and the pH dependency of reaction using Spm as a substrate

Fms1 was originally characterized in yeast as a high-copy suppressor of the antifungal drug fenpropimorph. Its cloning and production as recombinant enzyme facilitated the characterization of its substrate specificity in 2003 [31]. The enzyme has been crystallized with several ligands and their structural data are available [16]. APAO, SMOX and Fms1 share many common features but their substrate specificities differ interestingly. SMOX prefers Spm over N^1-AcSpm, and other polyamines or their acetylated derivatives are not substrates [40]. APAO prefers N^1-AcSpm, N^1,N^{12}-DiAcSpm and N^1-AcSpd while N^8-AcSpd is an efficient inhibitor for the enzyme [29,44]. Fms1 cleaves at the exo-N^4-site of N^1-AcSpm > Spm > N^1-AcSpd >> and endo-N^4-site of N^8-AcSpd [31]. Recent kinetic data of Fms1 by Adachi et al. [45] sets Spm (k_{cat} = 39.0 ± 1.5 s^{-1}) > N^1-AcSpm. (k_{cat} = 15.1 ± 0.4 s^{-1}). APAO and SMOX cleave substrates at exo-N^4-site, thus differentiating them from the maize PAO. Fms1 has the highest k_{cat} values for Spm in comparison with APAO or SMOX [25,29,31,45].

Here we used recombinant Fms1 having the activity of 30.9 ± 0.45 μmol/mg/min (k_{cat} = 30.3 ± 0.44 s^{-1}) in Glycine-NaOH buffer at pH 9.0 and with 1 mM Spm as a substrate (Table 3). The reaction velocity was slightly enhanced in 100 mM Tris/HCl or 170 mM Bis/Tris buffers at pH 9.0 reaching 36.1 ± 0.24 μmol/mg/min. The use of HPLC for detecting reaction products allowed a reliable determination of reaction velocity compared with pH which could be hampered in peroxidase-coupled assay systems [30]. Reaction velocity was the highest at pH 9.25 and was retarded to 60% at pH 8.5 and to ∼15% at pH 8.0 in comparison with reaction rate at the optimum pH (Supplementary Material 1, Figure S1). Determined pH dependency correlated with the data obtained by Adachi et al. [45]. The pH dependency of the reaction velocity was similar to that of APAO and SMOX [32,45-47]. The kinetic values of Fms1 for racemic Me_2Spm, *(R,R)*-Me_2Spm, *(S,S)*-Me_2Spm and Spm are shown in Table 3. Despite 1,12-bis-methylation, the affinities of analogues for Fms1 were retained but the catalytic velocities dropped to less than one tenth in comparison with Spm. Thus, Fms1 tolerated 1,12-bis-methyl substituents in spite of their stereoconfiguration in Spm poorly in

Table 3 Kinetic values for Spm and its 1,12-bis-methylated analogues as substrates of Fms1

Polyamine	K_m (μM)	V_{max} (μmol/min/mg)	k_{cat} (s^{-1})	k_{cat}/K_m (M^{-1} s^{-1})
Spm[1]	77 ± 8	31.7 ± 1.0	31.1 ± 0.98	(400 ± 38) × 10^3
Racemic Me_2Spm[2]	54 ± 7	1.51 ± 0.05	1.48 ± 0.05	(27 ± 3.7) × 10^3
(R,R)-Me_2Spm[3]	98 ± 12	0.79 ± 0.03	0.77 ± 0.03	(7.9 ± 1.1) × 10^3
(S,S)-Me_2Spm[3]	61 ± 7	1.89 ± 0.05	1.85 ± 0.05	(30 ± 3.6) × 10^3

Reactions were carried out in triplicates in 100 mM Glycine-NaOH buffer at pH 9.0 and analysed for reaction products as described in 'Experimental procedures' section. Turnover number (k_{cat}) has been calculated by using M_r of 58833 for Fms1 monomer.
[1]25, 50, 75, 100, 200, 400 and 600 μM concentrations were used.
[2]25, 50, 100, 200, 400 and 1000 μM concentrations were used.
[3]25, 50, 100, 200, 400, 600 and 1000 μM concentrations were used.

comparison with APAO and SMOX. In the case of APAO catalytic velocity using *(S,S)*-Me_2Spm was slightly enhanced in comparison with Spm. Specificity constant ratios in using *(S,S)*-Me_2Spm as a reference substrate between these polyamine oxidases are SMOX (SS/RR 454; SS/Spm 2.1)>>>APAO (SS/RR 28; SS/Spm 7.1)> Fms1 (SS/RR 3.9; SS/Spm 0.07) [25,29].

Control of regioselectivity of Fms1 for Spd with aldehydes

Aldehyde supplementation has been successfully used to mimic N^1-acetylation of Spd in APAO catalysis, since N^1-AcSpd is a substrate of Fms1. We studied the effects of different aldehydes on substrate properties of Spd for Fms1 [29,31]. First, we found that Fms1 slowly degraded Spd and the K_m value for Spd was expectedly much higher than that for Spm and N^1-AcSpd. The reaction was expected to yield Put and 3-aminopropanal, yet our HPLC analyses indicated that DAP was also produced (Table 4). This implies the presence of two cleavage sites, at exo- and at endo-N^4-sites of Spd as reported earlier for N^1- and N^8-AcSpd respectively [31]. Table 4 shows the effects of various aldehydes (mimicking N^1-AcSpd, N^8-AcSpd and N^1,N^8-DiAcSpd) on the Fms1-catalysed reaction with Spd as the substrate. Unlike the human APAO reaction, where the aldehydes mainly increased V_{max} values, in the Fms1 reaction the aldehydes most profoundly decreased the K_m values. Table 4 also shows the two distinct cleavage sites, cleavage at E1 yielding Put and at E2 yielding DAP. In the absence of the aldehydes, the E1 route was strongly preferred. Most of the aldehydes enhanced the cleavage at E1, yet three of them (A6, A18 and A4) shifted the balance towards E2 cleavage site (Table 4). The aldehydes increased the ratio of the cleavage pathways (E1/E2) up to 5-fold (A7) and decreased it up to 12-fold (A4) at best. In most cases, the supplemented aldehydes brought about a dramatic increase in the enzyme efficiency (k_{cat}/K_m) at both cleavage sites. However, with the tested aldehydes the maximal reaction velocities of 1/10 of k_{cat} for E1 (N^1-AcSpd) cleavage and approximately one-third for E2 (N^8-AcSpd) cleavage were reached respectively. Thus, in the case of Fms1 using Spd as a substrate the supplementation of aromatic aldehydes to reaction mixture gives a possibility to control the regioselectivity of the reaction.

N^1-AcMeSpd and its *(R)*- and *(S)*-enantiomers as substrates of Fms1

The human recombinant APAO readily catalysed oxidation of N^1-Ac-*(R)*-MeSpd and Schiff bases of MeSpd with aromatic aldehydes [24,29]. Unexpectedly, Fms1 did not metabolize neither of *(R)*- and *(S)*-enantiomers of N^1-Ac-MeSpds (Supplementary Material 1, Table S1). Accordingly, *(R)*- and *(S)*-MeSpd had similar (K_m > 500 μM) as Spd (Supplementary Material 1, Table S2). Above applies to both of the tested aldehydes A12 and A13 (50 and 500 μM) with 1 or 4 mM *(R-)* or *(S)*-MeSpd (Supplementary Material 1, Table S3).

Conclusion

The obtained data clearly demonstrate that Fms1 and APAO (both using achiral natural polyamines as substrates) appear to be representative examples of enzymes, whose stereospecificity and regioselectivity can be modulated by small guide molecules. Having established that Spd in Fms1 reaction has two cleavage sites, i.e. exo-N^4-site (E_1) and endo-N^4-site (E_2), it turned out to be possible to induce predominant cleavage at either (E_1) or (E_2) site by minor changes of the structure of supplemented aromatic aldehyde needed to form ***in situ*** a novel substrate—Schiff base with Spd. The same 'aldehyde approach' in the case of APAO and chiral 1-MeSpds' provided a unique possibility to induce cleavage of either *(R)*- or *(S)*-isomer depending on the structure of used aromatic aldehyde. Fms1 like APAO exhibits hidden stereospecificity and prefers *(S,S)*- to *(R,R)*-Me_2Spm diastereoisomer with notably lower k_{cat} in comparison with Spm. The present data together with earlier accumulated knowledge of polyamine analogue structure–bioactivity

Bioscience Reports (2018) **38** BSR20180527
https://doi.org/10.1042/BSR20180527

relationships allow deriving novel chemico-biological applications to modulate cell physiology and generation of specific substrates or inhibitors for polyamine metabolizing enzymes.

Table 4 Kinetic values of N^1-AcSpd, N^8-AcSpd, and Spd in the presence or absence of different aldehydes, for Fms1

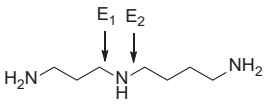

Substrate and/or supplementary aldehyde	Ratio of E_1/E_2	E_1 cleavage kinetic values (Put)			E_2 cleavage kinetic values (DAP)		
		K_m (μM)	k_{cat} (s^{-1})	k_{cat}/K_m ($M^{-1}s^{-1}$)	K_m (μM)	k_{cat} (s^{-1})	k_{cat}/K_m ($M^{-1}s^{-1}$)
N^1-AcSpd	NA	42 ± 8	65 ± 2	(1600 ± 300) × 10^3	NA	NA	NA
N^8-AcSpd	NA	NA	NA	NA	122 ± 18	1.4 ± 0.1	(12 ± 1.8) × 10^3
Spd	7.5	534 ± 36	0.34 ± 0.01	640 ± 47	643 ± 52	0.05 ± 0.00	86 ± 7
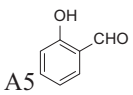 A5	5.2	25 ± 3	0.54 ± 0.01	(22 ± 2.6) × 10^3	18 ± 3	0.08 ± 0.00	(4.2 ± 0.8)×10^3
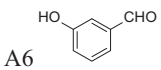 A6	0.22	32 ± 3	0.31 ± 0.01	(0.97 ± 0.10) × 10^3	107 ± 6	0.47 ± 0.01	(4.4 ± 0.3)×10^3
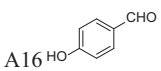 A16	118	1.3 ± 1.0	0.11 ± 0.00	(85 ± 65) × 10^3	42 ± 10	0.03 ± 0.00	(0.72 ± 0.17) × 10^3
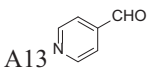 A13	12.9	139 ± 9	7.4 ± 0.2	(53 ± 3.8) × 10^3	47 ± 6	0.19 ± 0.01	(4.1 ± 0.6) × 10^3
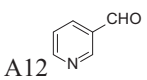 A12	8.0	138 ± 8	5.5 ± 0.1	(40 ± 2.4) × 10^3	96 ± 7	0.48 ± 0.01	(5.0 ± 0.4) × 10^3
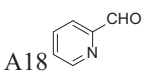 A18	2.2	25 ± 2	0.49 ± 0.01	(19 ± 1.6) × 10^3	55 ± 4	0.49 ± 0.01	(8.8 ± 0.7) × 10^3
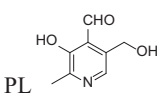 PL	NA	33 ± 3	1.13 ± 0.03	(34 ± 3.2) × 10^3	NA	NA	NA
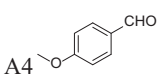 A4	NA	NA	0.13 ± 0.00	NA	217 ± 10	0.22 ± 0.00	(1.0 ± 0.05) × 10^3
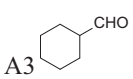 A3	5.4	185 ± 16	1.41 ± 0.04	(7.6 ± 0.7) × 10^3	296 ± 16	0.43 ± 0.01	(1.4 ± 0.09) × 10^3
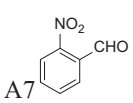 A7	NA	16 ± 3	1.06 ± 0.04	(66 ± 13) × 10^3	NA	0.03 ± 0.00	NA
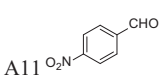 A11	6.4	5.3 ± 0.9	0.37 ± 0.00	(70 ± 12) × 10^3	4.7 ± 0.8	0.05 ± 0.00	(11 ± 1.8) × 10^3

The reactions were carried out in triplicate at pH 9.0 in 100 mM Glycine-NaOH at +25°C with the fixed 1 mM Spd supplemented with increasing concentrations (25, 50, 75, 100, 250, 500 and 1000 μM) of tested aldehyde (Figure 2). Kinetic values for Spd were determined by using substrate concentrations of 50, 100, 200, 400, 600, 1000 and 4000 μM. Recombinant Fms1 was 1–2 μg/reaction and the incubation time from 5 to 30 min. Linearity of reaction was monitored by using $T_{1/2}$ controls, i.e. samples that have been incubated for 2.5–15 min (half of the reaction time of an ordinary sample). N^1AcSpd 50, 100, 300, 600 and 1000 μM 0.05 μg of Fms1 at 25°C 1 min. N^8AcSpd 50, 100, 200 and 600 μM 0.59 μg of Fms1 at 25°C 10 min. Reaction mixtures without the enzyme supplement were used to control purity of the reagents and to exclude non-enzymatic degradation of the compounds. E_1 cleavage was monitored by HPLC by measuring Put formation and E_2 cleavage by determining DAP content. k_{cat} values have been calculated assuming M_r of 58833 for monomer with one catalytically active centre.

Acknowledgements

We thank Ms Tuula Reponen for HPLC analysis and technical assistance, Ms Anne Karppinen and Ms Arja Korhonen for technical assistance and Ms Maritta Salminkoski for the purification of aldehydes used for the study.

Competing interests

The authors declare that there are no competing interests associated with the manuscript.

Author contribution

L.A. and T.A.K planned the experiments and constructed the study. T.A.K. and M.T.H. carried out the enzyme kinetics experiments and calculated the results. N.G., A.R.K. and J.V. synthesized the polyamine analogues and analysed their purity. Q.H. provided the recombinant Fms1 enzyme protein and the expression vector of Fms1 for recombinant protein production. A.U. prepared the recombinant APAO and SMOX. All the authors took part in data analysis and in writing the manuscript.

Funding

This work was supported by the Academy of Finland [grant numbers 266196, 315487]; the University of Eastern Finland Strategic Spearhead Funding [grant number Dnro;197.02.05.02.11]; the Russian Science Foundation [grant number #17-74-20049 (to A.R.K.)]; and the Program of Fundamental Research for State Academies for years 2013–2020 [grant number #01201363818].

Abbreviations

APAO, acetylpolyamine oxidase; DAP, 1,3-diaminopropane; DHS, deoxyhypusine synthase; Fms1, yeast polyamine oxidase; MeSpd, 1-methylspermidine (1,8-diamino-5-azanonane); Me_2Spm, 1,12-bis-methylspermine (2,13-diamino-5,10-diazatetradecane); Put, putrescine; SMOX, spermine oxidase; Spd, spermidine; Spm, spermine; SSAT, Spd/Spm-N^1-acetyltransferase.

References

1 Tabor, C.W. and Tabor, H. (1984) Polyamines. *Annu. Rev. Biochem.* **53**, 749–790, https://doi.org/10.1146/annurev.bi.53.070184.003533
2 Wallace, H.M., Fraser, A.V. and Hughes, A. (2003) A perspective of polyamine metabolism. *Biochem. J.* **376**, 1–14, https://doi.org/10.1042/bj20031327
3 Palmer, A.J. and Wallace, H.M. (2010) The polyamine transport system as a target for anticancer drug development. *Amino Acids* **38**, 415–422, https://doi.org/10.1007/s00726-009-0400-2
4 Seiler, N. (1987) Functions of polyamine acetylation. *Can. J. Physiol. Pharmacol.* **65**, 2024–2035, https://doi.org/10.1139/y87-317
5 Vujcic, S., Diegelman, P., Bacchi, C.J., Kramer, D.L. and Porter, C.W. (2002) Identification and characterization of a novel flavin-containing spermine oxidase of mammalian cell origin. *Biochem. J.* **367**, 665–675, https://doi.org/10.1042/bj20020720
6 Casero, R.A. and Pegg, A.E. (2009) Polyamine catabolism and disease. *Biochem. J.* **421**, 323–338, https://doi.org/10.1042/BJ20090598
7 Murray-Stewart, T.R., Woster, P.M. and Casero, Jr, R.A. (2016) Targeting polyamine metabolism for cancer therapy and prevention. *Biochem. J.* **473**, 2937–2953, https://doi.org/10.1042/BCJ20160383
8 Birkholtz, L.M., Williams, M., Niemand, J., Louw, A.I., Persson, L. and Heby, O. (2011) Polyamine homoeostasis as a drug target in pathogenic protozoa: peculiarities and possibilities. *Biochem. J.* **438**, 229–244, https://doi.org/10.1042/BJ20110362
9 Babbar, N., Murray-Stewart, T. and Casero, Jr, R.A. (2007) Inflammation and polyamine catabolism: the good, the bad and the ugly. *Biochem. Soc. Trans.* **35**, 300–304, https://doi.org/10.1042/BST0350300
10 Lawson, K.R., Marek, S., Linehan, J.A., Woster, P.M., Casero, Jr, R.A., Payne, C.M. et al. (2002) Detoxification of the polyamine analogue N^1-ethyl-N^{11}-[(cycloheptyl)methy]-4,8-diazaundecane (CHENSpm) by polyamine oxidase. *Clin. Cancer Res.* **8**, 1241–1247
11 Pledgie, A., Huang, Y., Hacker, A., Zhang, Z., Woster, P.M., Davidson, N.E. et al. (2005) Spermine oxidase SMO(PAOh1), Not N^1-acetylpolyamine oxidase PAO, is the primary source of cytotoxic H_2O_2 in polyamine analogue-treated human breast cancer cell lines. *J. Biol. Chem.* **280**, 39843–39851, https://doi.org/10.1074/jbc.M508177200
12 Sjogren, T., Wassvik, C.M., Snijder, A., Aagaard, A., Kumanomidou, T., Barlind, L. et al. (2017) The structure of murine N(1)-acetylspermine oxidase reveals molecular details of vertebrate polyamine catabolism. *Biochemistry* **56**, 458–467, https://doi.org/10.1021/acs.biochem.6b01140
13 Tavladoraki, P., Cervelli, M., Antonangeli, F., Minervini, G., Stano, P., Federico, R. et al. (2011) Probing mammalian spermine oxidase enzyme-substrate complex through molecular modeling, site-directed mutagenesis and biochemical characterization. *Amino Acids* **40**, 1115–1126, https://doi.org/10.1007/s00726-010-0735-8
14 Tormos, J.R., Henderson Pozzi, M. and Fitzpatrick, P.F. (2012) Mechanistic studies of the role of a conserved histidine in a mammalian polyamine oxidase. *Arch. Biochem. Biophys.* **528**, 45–49, https://doi.org/10.1016/j.abb.2012.08.007
15 Binda, C., Angelini, R., Federico, R., Ascenzi, P. and Mattevi, A. (2001) Structural bases for inhibitor binding and catalysis in polyamine oxidase. *Biochemistry* **40**, 2766–2776, https://doi.org/10.1021/bi002751j
16 Huang, Q., Liu, Q. and Hao, Q. (2005) Crystal structures of Fms1 and its complex with spermine reveal substrate specificity. *J. Mol. Biol.* **348**, 951–959, https://doi.org/10.1016/j.jmb.2005.03.008

17 Moriya, S.S., Miura, T., Takao, K., Sugita, Y., Samejima, K., Hiramatsu, K. et al. (2014) Development of irreversible inactivators of spermine oxidase and N^1-acetylpolyamine oxidase. *Biol. Pharm. Bull.* **37**, 475–480, https://doi.org/10.1248/bpb.b13-00913
18 Blaschko, H. (1952) Amine oxidase and amine metabolism. *Pharmacol. Rev.* **4**, 415–458
19 Barreiro, E.J., Kummerle, A.E. and Fraga, C.A. (2011) The methylation effect in medicinal chemistry. *Chem. Rev.* **111**, 5215–5246, https://doi.org/10.1021/cr200060g
20 Lakanen, J.R., Coward, J.K. and Pegg, A.E. (1992) alpha-Methyl polyamines: metabolically stable spermidine and spermine mimics capable of supporting growth in cells depleted of polyamines. *J. Med. Chem.* **35**, 724–734, https://doi.org/10.1021/jm00082a013
21 Byers, T.L., Lakanen, J.R., Coward, J.K. and Pegg, A.E. (1994) The role of hypusine depletion in cytostasis induced by S-adenosyl-L-methionine decarboxylase inhibition: new evidence provided by 1- methylspermidine and 1,12-dimethylspermine. *Biochem. J.* **303**, 363–368, https://doi.org/10.1042/bj3030363
22 Järvinen, A., Grigorenko, N., Khomutov, A.R., Hyvönen, M.T., Uimari, A., Vepsäläinen, J. et al. (2005) Metabolic stability of alpha-methylated polyamine derivatives and their use as substitutes for the natural polyamines. *J. Biol. Chem.* **280**, 6595–6601, https://doi.org/10.1074/jbc.M412788200
23 Keinänen, T.A., Järvinen, A., Uimari, A., Vepsäläinen, J., Khomutov, A.R., Grigorenko, N.A. et al. (2007) Alpha-methylated polyamines as potential drugs and experimental tools in enzymology. *Mini Rev. Med. Chem.* **7**, 813–820, https://doi.org/10.2174/138955707781387867
24 Järvinen, A.J., Cerrada-Gimenez, M., Grigorenko, N.A., Khomutov, A.R., Vepsäläinen, J.J., Sinervirta, R.M. et al. (2006) Alpha-Methyl polyamines: Efficient synthesis and tolerance studies *in vivo* and *in vitro*. First evidence for dormant stereospecificity of polyamine oxidase. *J. Med. Chem.* **49**, 399–406
25 Hyvönen, M.T., Keinänen, T.A., Cerrada-Gimenez, M., Sinervirta, R., Grigorenko, N., Khomutov, A.R. et al. (2007) Role of hypusinated eukaryotic translation initiation factor 5A in polyamine depletion-induced cytostasis. *J. Biol. Chem.* **282**, 34700–34706, https://doi.org/10.1074/jbc.M704282200
26 Hyvönen, M.T., Keinänen, T.A., Khomutov, M., Simonian, A., Vepsäläinen, J., Park, J.H. et al. (2012) Effects of novel C-methylated spermidine analogs on cell growth via hypusination of eukaryotic translation initiation factor 5A. *Amino Acids* **42**, 685–695, https://doi.org/10.1007/s00726-011-0984-1
27 Hyvönen, M.T., Howard, M.T., Anderson, C.B., Grigorenko, N., Khomutov, A.R., Vepsäläinen, J. et al. (2009) Divergent regulation of the key enzymes of polyamine metabolism by chiral alpha-methylated polyamine analogues. *Biochem. J.* **422**, 321–328, https://doi.org/10.1042/BJ20090737
28 Hyvönen, M.T., Khomutov, M., Petit, M., Weisell, J., Kochetkov, S.N., Alhonen, L. et al. (2015) Enantiomers of 3-methylspermidine selectively modulate deoxyhypusine synthesis and reveal important determinants for spermidine transport. *ACS Chem. Biol.* **10**, 1417–1424, https://doi.org/10.1021/cb500938e
29 Järvinen, A., Keinänen, T.A., Grigorenko, N.A., Khomutov, A.R., Uimari, A., Vepsäläinen, J. et al. (2006) Guide molecule-driven stereospecific degradation of alpha-methylpolyamines by polyamine oxidase. *J. Biol. Chem.* **281**, 4589–4595, https://doi.org/10.1074/jbc.M509959200
30 Hyvönen, T., Keinänen, T.A., Khomutov, A.R., Khomutov, R.M. and Eloranta, T.O. (1992) Monitoring of the uptake and metabolism of aminooxy analogues of polyamines in cultured cells by high-performance liquid chromatography. *J. Chromatogr.* **574**, 17–21, https://doi.org/10.1016/0378-4347(92)80093-6
31 Landry, J. and Sternglanz, R. (2003) Yeast Fms1 is a FAD-utilizing polyamine oxidase. *Biochem. Biophys. Res. Commun.* **303**, 771–776, https://doi.org/10.1016/S0006-291X(03)00416-9
32 Hölttä, E. (1977) Oxidation of spermidine and spermine in rat liver: purification and properties of polyamine oxidase. *Biochemistry* **16**, 91–100, https://doi.org/10.1021/bi00620a015
33 Wang, Y., Devereux, W., Woster, P.M., Stewart, T.M., Hacker, A. and Casero, Jr, R.A. (2001) Cloning and characterization of a human polyamine oxidase that is inducible by polyamine analogue exposure. *Cancer Res.* **61**, 5370–5373
34 Vujcic, S., Liang, P., Diegelman, P., Kramer, D.L. and Porter, C.W. (2003) Genomic identification and biochemical characterization of the mammalian polyamine oxidase involved in polyamine back-conversion. *Biochem. J.* **370**, 19–28, https://doi.org/10.1042/bj20021779
35 Cervelli, M., Bellini, A., Bianchi, M., Marcocci, L., Nocera, S., Polticelli, F. et al. (2004) Mouse spermine oxidase gene splice variants. Nuclear subcellular localization of a novel active isoform. *Eur. J. Biochem.* **271**, 760–770, https://doi.org/10.1111/j.1432-1033.2004.03979.x
36 Murray-Stewart, T., Wang, Y., Goodwin, A., Hacker, A., Meeker, A. and Casero, Jr, R.A. (2008) Nuclear localization of human spermine oxidase isoforms - possible implications in drug response and disease etiology. *FEBS J.* **275**, 2795–2806, https://doi.org/10.1111/j.1742-4658.2008.06419.x
37 Chaturvedi, R., Asim, M., Romero-Gallo, J., Barry, D.P., Hoge, S., de Sablet, T. et al. (2011) Spermine oxidase mediates the gastric cancer risk associated with *Helicobacter pylori* CagA. *Gastroenterology* **141**, 1696–1708.e1691-1692, https://doi.org/10.1053/j.gastro.2011.07.045
38 Goodwin, A.C., Jadallah, S., Toubaji, A., Lecksell, K., Hicks, J.L., Kowalski, J. et al. (2008) Increased spermine oxidase expression in human prostate cancer and prostatic intraepithelial neoplasia tissues. *Prostate* **68**, 766–772, https://doi.org/10.1002/pros.20735
39 Goodwin, A.C., Destefano Shields, C.E., Wu, S., Huso, D.L., Wu, X., Murray-Stewart, T.R. et al. (2011) Polyamine catabolism contributes to enterotoxigenic *Bacteroides fragilis*-induced colon tumorigenesis. *Proc. Natl. Acad. Sci. U.S.A.* **108**, 15354–15359, https://doi.org/10.1073/pnas.1010203108
40 Wang, Y., Murray-Stewart, T., Devereux, W., Hacker, A., Frydman, B., Woster, P.M. et al. (2003) Properties of purified recombinant human polyamine oxidase, PAOh1/SMO. *Biochem. Biophys Res. Commun.* **304**, 605–611, https://doi.org/10.1016/S0006-291X(03)00636-3
41 Seiler, N., Bolkenius, F.N., Knödgen, B. and Mamont, P. (1980) Polyamine oxidase in rat tissues. *Biochim. Biophys. Acta* **615**, 480–488, https://doi.org/10.1016/0005-2744(80)90514-8
42 Suzuki, O., Matsumoto, T. and Katsumata, Y. (1984) Determination of polyamine oxidase activities in human tissues. *Experientia* **40**, 838–839, https://doi.org/10.1007/BF01951981
43 Keinänen, T.A., Hyvönen, M.T., Alhonen, L., Vepsäläinen, J. and Khomutov, A.R. (2014) Selective regulation of polyamine metabolism with methylated polyamine analogues. *Amino Acids* **46**, 605–620, https://doi.org/10.1007/s00726-013-1587-9
44 Bolkenius, F.N. and Seiler, N. (1981) Acetylderivatives as intermediates in polyamine catabolism. *Int. J. Biochem.* **13**, 287–292, https://doi.org/10.1016/0020-711X(81)90080-X

45 Adachi, M.S., Torres, J.M. and Fitzpatrick, P.F. (2010) Mechanistic studies of the yeast polyamine oxidase Fms1: kinetic mechanism, substrate specificity, and pH dependence. *Biochemistry* **49**, 10440–10448, https://doi.org/10.1021/bi1016099

46 Henderson Pozzi, M., Gawandi, V. and Fitzpatrick, P.F. (2009) pH dependence of a mammalian polyamine oxidase: insights into substrate specificity and the role of lysine 315. *Biochemistry* **48**, 1508–1516, https://doi.org/10.1021/bi802227m

47 Häkkinen, M.R., Hyvönen, M.T., Auriola, S., Casero, Jr, R.A., Vepsäläinen, J., Khomutov, A.R. et al. (2010) Metabolism of N-alkylated spermine analogues by polyamine and spermine oxidases. *Amino Acids* **38**, 369–381, https://doi.org/10.1007/s00726-009-0429-2

Supplementary Material 1

Controlling the regioselectivity and stereospecificity of FAD-dependent polyamine oxidases with the use of amine-attached guide molecules as conformational modulators

Tuomo A. Keinänen*[,1], Nikolay Grigorenko[‡], Alex R. Khomutov[§], Qingqiu Huang[†], Anne Uimari[|], Leena Alhonen*, Mervi T. Hyvönen* and Jouko Vepsäläinen*

**School of Pharmacy, Biocenter Kuopio, University of Eastern Finland, Kuopio Campus, P.O. Box 1627 Kuopio, FI-70211 Finland. [|]Natural Resources Institute Finland, Neulaniementie 5, FI-70210 Kuopio, Finland. [†]MacCHESS at the Cornell High Energy Synchrotron Source, Cornell University Ithaca, NY 14853-8001, USA. [‡]BASF Schweiz AG, P.O. Box, CH 4002, Basel, Switzerland. [§]Engelhardt Institute of Molecular Biology, Russian Academy of Sciences, Vavilov St 32, 119991 Moscow, Russia.*

[1] Corresponding author Tuomo.Keinanen@uef.fi

Abbreviations:

Fms1, yeast polyamine oxidase; MeSpd, 1-methylspermidine (1,8-diamino-5-azanonane); Me_2Spm, 1,12-dimethylspermine (2,13-Diamino-5,10-diazatetradecane); N^1-Ac-MeSpd, N^8-Acetyl-1,8-diamino-5-azanonane.

Supplementary Table 1. N^1-AcSpd and N^1-Acetylated MeSpd as substrates of Fms1.

The reactions were carried out in triplicate at pH 9.0 in 100 mM Glycine-NaOH at +25°C. Kinetic values for N^1-Ac-MeSpd enantiomers were determined by using substrate concentrations of 25, 50, 100, 200, 400, 600 and 1000 μM. Recombinant Fms1 was 1.8 μg/reaction and the incubation times for Rac-MeSpd 30 min, (*R*)-MeSpd 20 min and (*S*)-MeSpd 40 minutes. Linearity of reaction was monitored by using $T_{1/2}$ controls, i.e. samples that have been incubated for 15, 10 and 20 min, respectively (half of the reaction time of an ordinary sample). Put formation was monitored by using HPLC. k_{cat} values have been calculated assuming M_r of 58,833 for monomer with one catalytically active centre.

Polyamine	**K_m (μM)**	**V_{max} (nmol/min/mg)**	**k_{cat} s^{-1}**	**k_{cat}/K_m $M^{-1}s^{-1}$**
N^1-AcSpd	42 ± 8	66,600 ± 2,300	65 ± 2	(1.56 ± 0.30) ×10^6
N^1-Ac-MeSpd	140 ± 23	50 ± 3	0.05 ± 0.00	357 ± 61
N^1-Ac-*(R)*-MeSpd	155 ± 29	61 ± 4	0.06 ± 0.00	387 ± 76
N^1-Ac-*(S)*-MeSpd	109 ± 18	22 ± 1	0.02 ± 0.00	183 ± 32

Supplementary Table 2 Enantiomers of MeSpd as substrates of Fms1.

The reactions were carried out in triplicate at pH 9.0 in 100 mM Glycine-NaOH at +25°C. Kinetic values for MeSpd enantiomers were determined by using substrate concentrations of 100, 300, 600, 1000, 2000 and 4000 μM. Recombinant Fms1 was 3.8 μg/reaction and the incubation time 60 minutes. Linearity of reaction was monitored by using $T_{1/2}$ controls, i.e. samples that have been incubated for 30 min (half of the reaction time of an ordinary sample). E_1 cleavage was monitored by HPLC by measuring Put formation and E_2 cleavage by determining butane-1,3-diamine content. k_{cat} values have been calculated assuming M_r of 58,833 for monomer with one catalytically active centre.

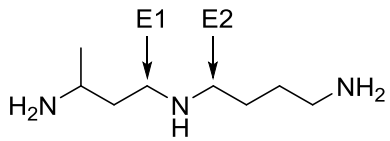	**E_1 cleavage kinetic values**			**E_2 cleavage kinetic values**		
Substrate	K_m (μM)	k_{cat} s^{-1}	k_{cat}/ K_m	K_m (μM)	k_{cat} s^{-1}	k_{cat}/ K_m
(R)-MeSpd	502 ± 31	0.014 ± 0	28 ± 2	467 ± 87	0.006 ± 0	13 ± 3
(S)-MeSpd	555 ± 33	0.011 ± 0	20 ± 1	606 ± 99	0.013 ± 0	22 ± 4

Supplementary Table 3 The effects of increasing aromatic aldehyde concentration for the regioselectivity of Fms1 using *(R)*-MeSpd or *(S)*-MeSpd as a substrate.

The reactions were carried out in triplicate at pH 9.0 in 100 mM Glycine-NaOH at +25°C with the fixed 1 or 4 mM MeSpd supplemented with increasing concentration 50 or 500 μM of tested aldehyde. Recombinant Fms1 was 1.6 μg/reaction and the incubation time from 15 to 30 minutes. Linearity of reaction was monitored by using $T_{1/2}$ controls, i.e. samples that have been incubated for 7.5 to 15 min (half of the reaction time of an ordinary sample). E_1 cleavage was monitored by HPLC by measuring Put formation and E_2 cleavage by determining butane-1,3-diamine content.

Substrate		*(R)*-MeSpd		*(S)*-MeSpd	
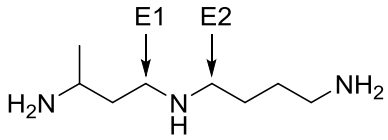		E1 *(nmol/mg/min)*	E2 *(nmol/mg/min)*	E1 *(nmol/mg/min)*	E2 *(nmol/mg/min)*
Without aldehyde 1 mM		9.5 ± 0.1	4.3 ± 0.9	7.2 ± 0.2	7.9 ± 1.1
Without aldehyde **4 mM**		**12.5 ± 0.0**	**5.6 ± 0.4**	**9.6 ± 0.1**	**11.1 ± 1.8**
aldehyde	*(μM)*				
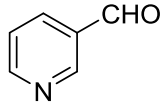 A12	50	10.5 ± 1.1	33.7 ± 4.8	29 ± 1.0	20.2 ± 1.0
	50	14.0 ± 0.9	31.8 ± 4.3	31 ± 1.8	23.3 ± 2.0
	500	12.7 ± 1.6	186 ± 24	57 ± 1.1	36 ± 4.2
	500	14.4 ± 0.8	216 ± 31	62 ± 3	41 ± 2.5
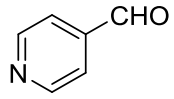 A13	50	19.1 ± 1.0	10.3 ± 3.1	45.6 ± 2.6	8.6 ± 1.8
	50	19.1 ± 0.4	9.6 ± 2.2	44.0 ± 1.2	10.0 ± 0.6
	500	72.8 ± 2.3	41.5 ± 3.4	66.1 ± 0.0	6.9 ± 0.7
	500	63.1 ± 1.0	39.5 ± 2.1	73.5 ± 0.4	7.4 ± 1.3

Supplementary Figure 1

Catalytic velocities of Fms1 with 1 mM Spm as a substrate in 170 mM Bis-Tris buffer at different pH

200 mM (170 mM in the final reaction mixtures) Bis-Tris propane buffer was prepared at pH 7.4; 8.0; 8.5; 8.8; 9.0; 9.2 and 9.5. Fms1 0.1 µg/reaction mixture was supplemented with 1 mM Spm at various pH V_{tot} 180 µl. Reaction mixtures were incubated at 25 °C water bath for four minutes until 20 µl of 50 % w/v SSA containing 100 uM DAH was added and vortexed briefly and placed on ice. HPLC was used to analyse Spd content of samples as described in Experimental Procedures. Values are averages of triplicate determinations expressed as µmol/min ± SD (error bars).

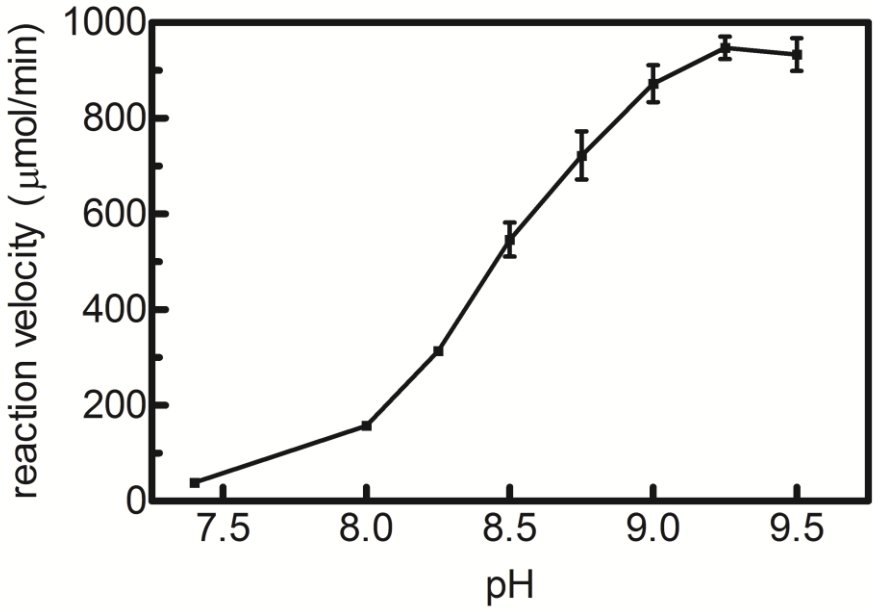

Supplementary Material 2

Controlling the regioselectivity and stereospecificity of FAD-dependent polyamine oxidases with the use of amine-attached guide molecules as conformational modulators

Tuomo A. Keinänen*[,1], Nikolay Grigorenko[‡], Alex R. Khomutov[§], Qingqiu Huang[†], Anne Uimari[ǁ], Leena Alhonen*, Mervi T. Hyvönen* and Jouko Vepsäläinen*

**School of Pharmacy, Biocenter Kuopio, University of Eastern Finland, Kuopio Campus, P.O. Box 1627 Kuopio, FI-70211 Finland. [ǁ]Natural Resources Institute Finland, Neulaniementie 5, FI-70210 Kuopio, Finland. [†]MacCHESS at the Cornell High Energy Synchrotron Source, Cornell University Ithaca, NY 14853-8001, USA. [‡]BASF Schweiz AG, P.O. Box, CH 4002, Basel, Switzerland. [§]Engelhardt Institute of Molecular Biology, Russian Academy of Sciences, Vavilov St 32, 119991 Moscow, Russia.*

[1] Corresponding author Tuomo.Keinanen@uef.fi

Michaelis-Menten Graphs and Data of Table 1

GraphPad Prism 5.03	N^1AcSpd	Bn-R-MeSpd	Bn-S-MeSpd	Bz-R-MeSpd	Bz-S-MeSpd	P4-R-MeSpd	P4-S-MeSpd
	µmol/min/mg	µmol/min/mg	µmol/min/mg	µmol/min/mg	µmol/min/mg	µmol/min/mg	µmol/min/mg
Michaelis-Menten							
Best-fit values							
V_{max}	2.969	0.1534	0.0307	5.017	0.02985	5.593	0.01522
K_m	8.218	2.039	1.639	1.214	0.2098	3.645	0.839
Std. Error							
V_{max}	0.02437	0.001549	0.001783	0.5122	0.000935	0.2399	0.0003134
K_m	0.3908	0.109	0.591	0.7426	0.161	0.5973	0.1498
95% Confidence Intervals							
V_{max}	2.901 to 3.037	0.1467 to 0.1600	0.02303 to 0.03838	3.387 to 6.647	0.02687 to 0.03282	4.928 to 6.259	0.01435 to 0.01609
K_m	7.133 to 9.303	1.570 to 2.508	0.0 to 4.182	0.0 to 3.577	0.0 to 0.7221	1.987 to 5.303	0.4233 to 1.255
Goodness of Fit							
Degrees of Freedom	4	2	2	3	3	4	4
R square	0.9962	0.9962	0.8491	0.6415	0.385	0.9614	0.9165
Absolute Sum of Squares	0.003966	0.000002157	0.000003144	0.7509	0.000003943	0.2719	0.0000007842
Sy.x	0.03149	0.001038	0.001254	0.5003	0.001146	0.2607	0.0004428
Constraints							
K_m	Km > 0.0	Km > 0.0	Km > 0.0	Km > 0.0	Km > 0.0	Km > 0.0	Km > 0.0
Number of points							
Analyzed	6	4	4	5	5	6	6

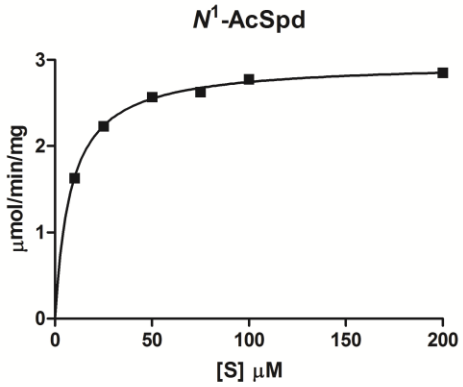
N^1-AcSpd
μmol/min/mg
[S] μM

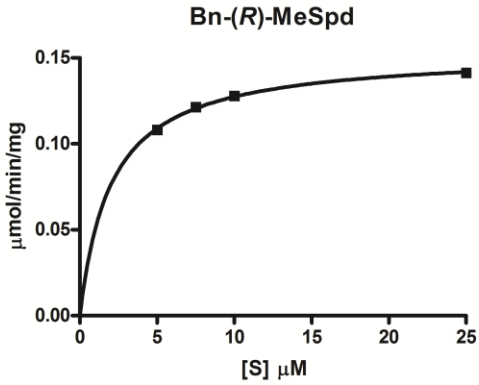
Bn-(R)-MeSpd
μmol/min/mg
[S] μM

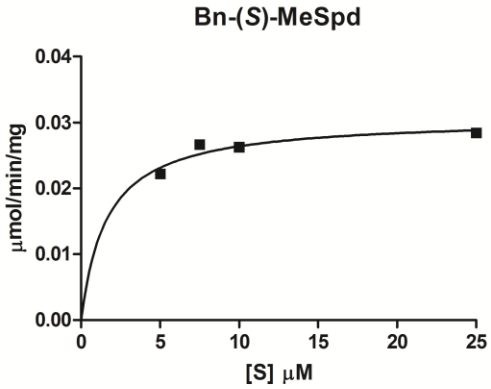
Bn-(S)-MeSpd
μmol/min/mg
[S] μM

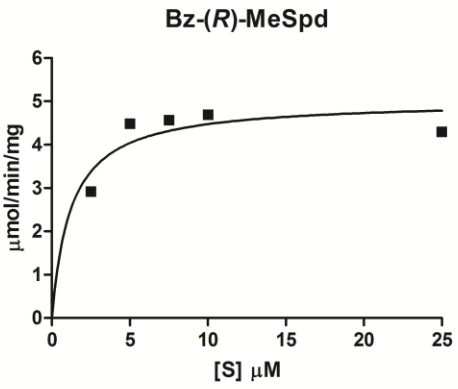
Bz-(R)-MeSpd
μmol/min/mg
[S] μM

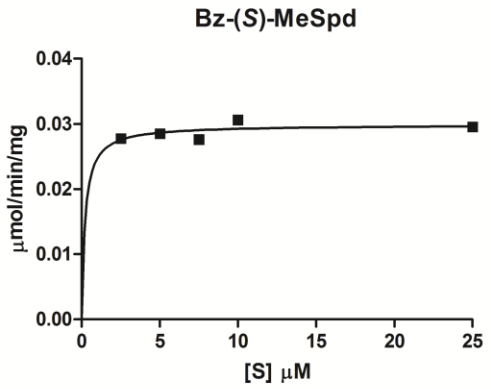
Bz-(S)-MeSpd
μmol/min/mg
[S] μM

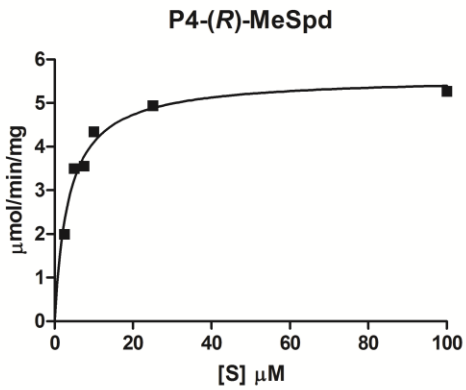
P4-(R)-MeSpd
μmol/min/mg
[S] μM

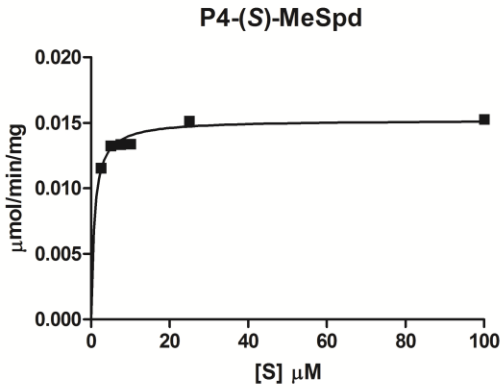
P4-(S)-MeSpd
μmol/min/mg
[S] μM

Michaelis-Menten Graphs and Data of Table 3

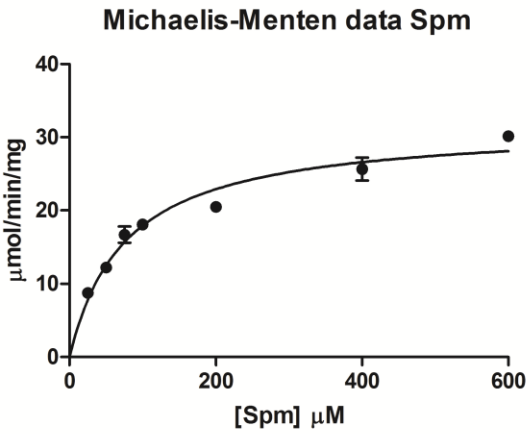

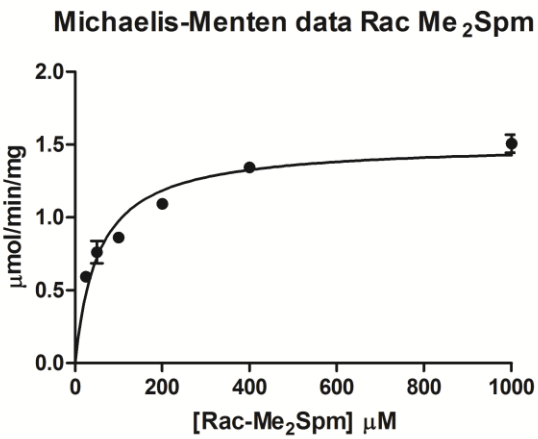

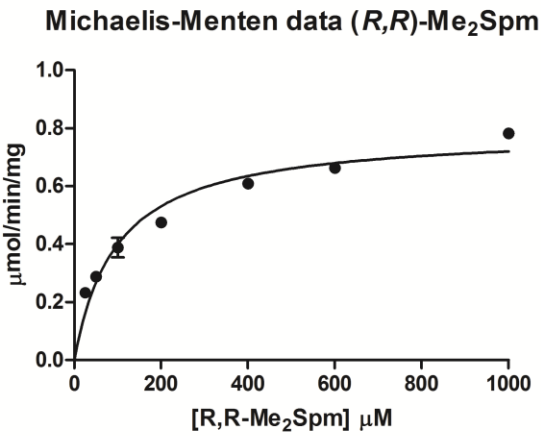

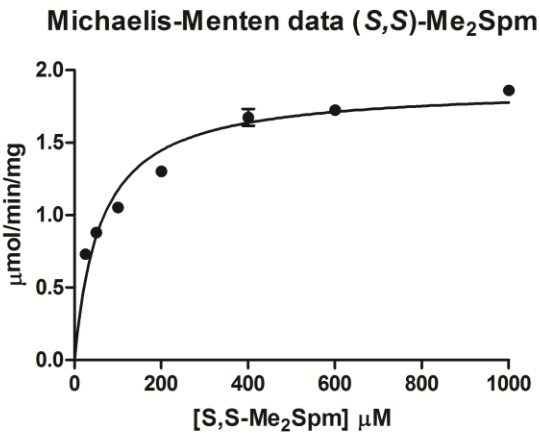

GraphPad Prism 5.03	Spm	Rac-Me_2Spm	(*R,R*)-Me_2Spm	(*S,S*)-Me_2Spm
	µmol/min/mg	µmol/min/mg	µmol/min/mg	µmol/min/mg
Michaelis-Menten				
Best-fit values				
V_{max}	31.71	1.506	0.7903	1.886
K_m	76.85	54.4	97.9	60.81
Std. Error				
V_{max}	1.030	0.05122	0.02751	0.05232
Km	7.842	7.168	12.37	7.038
95% Confidence Intervals				
V_{max}	29.55 to 33.86	1.397 to 1.614	0.7327 to 0.8479	1.777 to 1.996
K_m	60.43 to 93.26	39.20 to 69.60	72.02 to 123.8	46.08 to 75.54
Goodness of Fit				
Degrees of Freedom	19	16	19	19
R square	0.9511	0.9181	0.9392	0.9321
Absolute Sum of Squares	48.65	0.1543	0.04538	0.2437
Sy.x	1.600	0.09819	0.04887	0.1133
Constraints				
K_m	Km > 0.0	Km > 0.0	Km > 0.0	Km > 0.0
Number of points				
Analyzed	21	18	21	21

Michaelis-Menten Graphs and Data of Table 4 (N^1-AcSpd data shown in Supplementary 1 Table1)

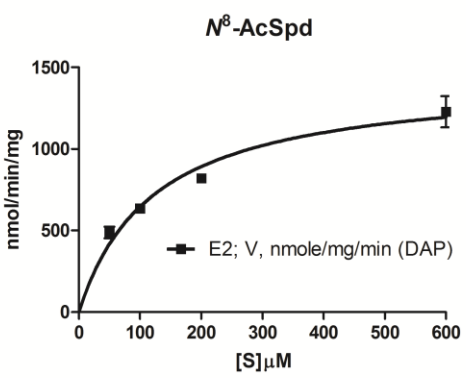

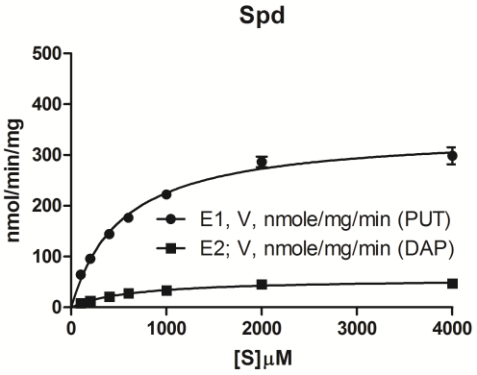

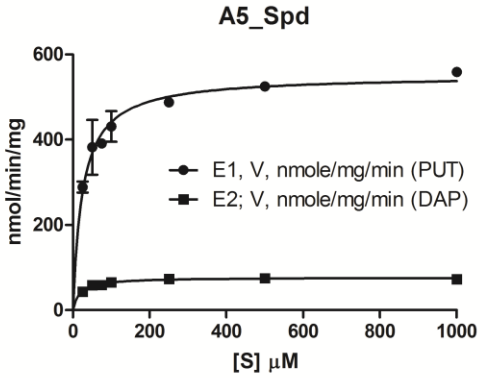

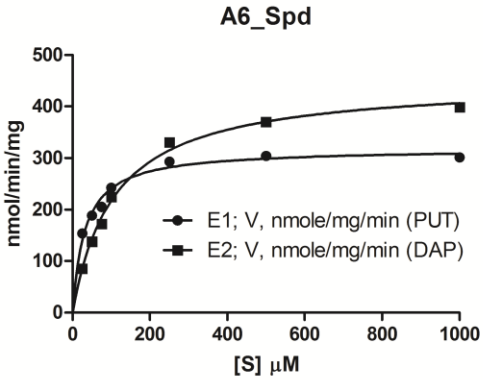

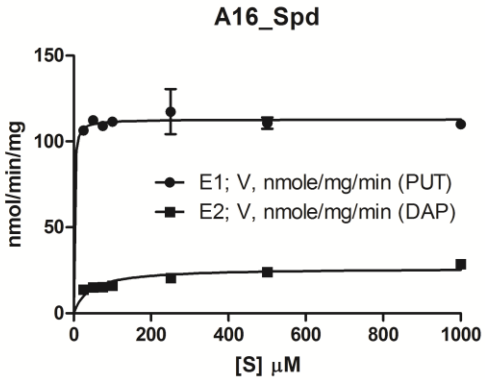

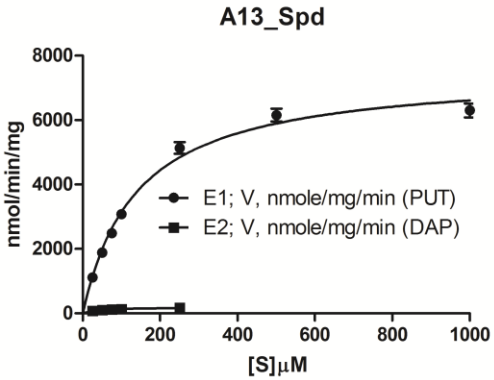

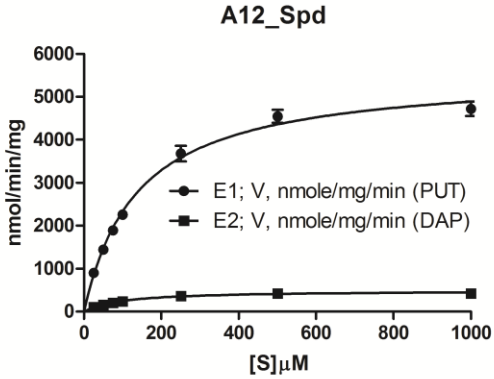

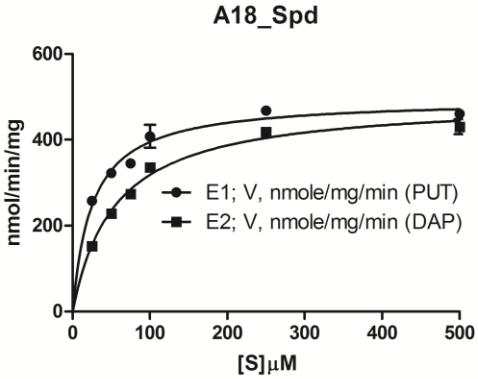

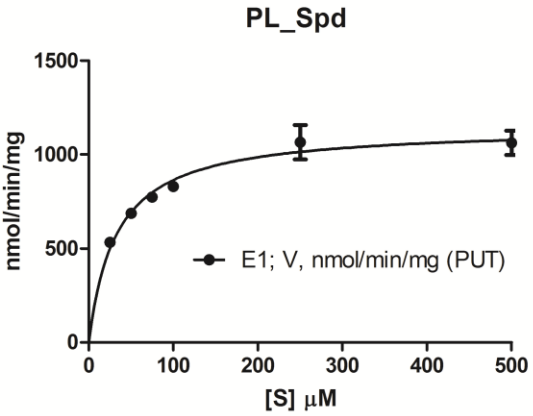
PL_Spd
nmol/min/mg
1500
1000
500
0
0
100
200
300
400
500
[S] μM
E1; V, nmol/min/mg (PUT)

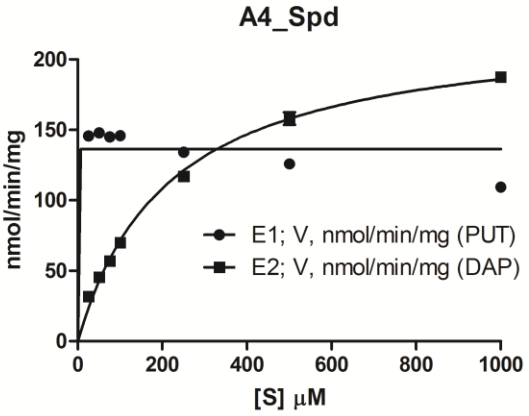
A4_Spd
nmol/min/mg
200
150
100
50
0
0
200
400
600
800
1000
[S] μM
E1; V, nmol/min/mg (PUT)
E2; V, nmol/min/mg (DAP)

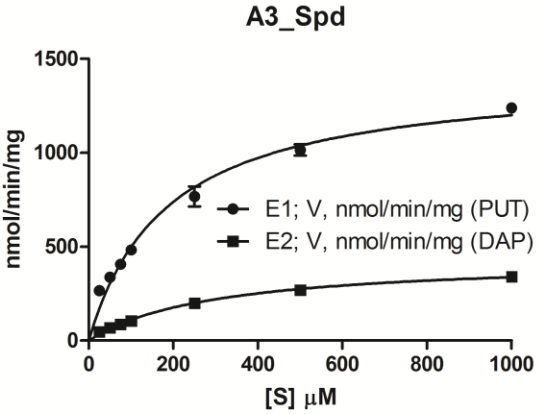
A3_Spd
nmol/min/mg
1500
1000
500
0
0
200
400
600
800
1000
[S] μM
E1; V, nmol/min/mg (PUT)
E2; V, nmol/min/mg (DAP)

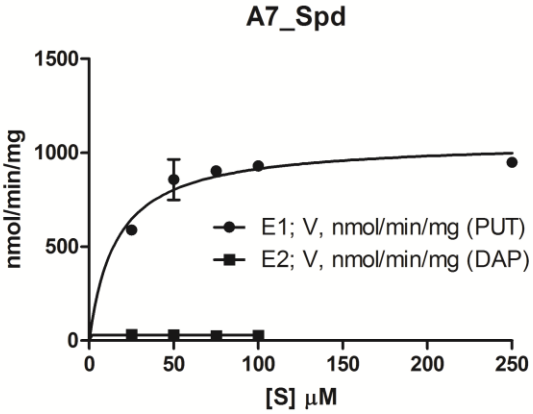
A7_Spd
nmol/min/mg
1500
1000
500
0
0
50
100
150
200
250
[S] μM
E1; V, nmol/min/mg (PUT)
E2; V, nmol/min/mg (DAP)

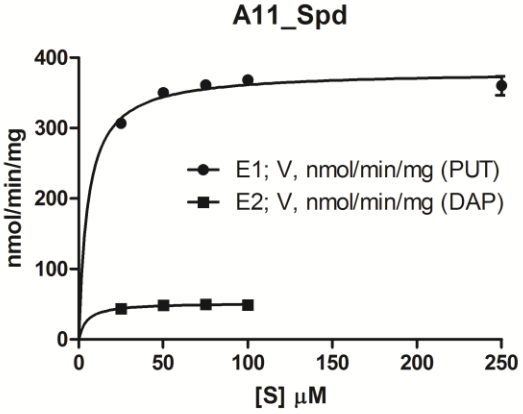
A11_Spd
nmol/min/mg
400
300
200
100
0
0
50
100
150
200
250
[S] μM
E1; V, nmol/min/mg (PUT)
E2; V, nmol/min/mg (DAP)

GraphPad Prism 5.03	N^8AcSpd	Spd E1	Spd E2	A5_Spd E1	A5_Spd E2	A6_Spd E1	A6_Spd E2
	nmol/min/mg	nmol/min/mg	nmol/min/mg	nmol/min/mg	nmol/min/mg	nmol/min/mg	nmol/min/mg
Michaelis-Menten					E1	E2	E1
Best-fit values							
V_{max}	1438	345.8	56.29	550.5	76.72	318.1	450.0
K_m	122.5	533.9	642.8	24.87	17.86	32.06	107.2
Std. Error							
V_{max}	78.14	7.799	1.627	13.54	1.878	5.977	7.656
K_m	18.36	35.89	52.36	3.075	2.595	2.710	5.632
95% Confidence Intervals							
V_{max}	1264 to 1612	329.5 to 362.2	52.88 to 59.69	521.1 to 580.0	72.63 to 80.81	305.1 to 331.1	433.3 to 466.6
K_m	81.60 to 163.4	458.8 to 609.0	533.2 to 752.4	18.17 to 31.57	12.20 to 23.51	26.16 to 37.97	94.89 to 119.4
Goodness of Fit							
Degrees of Freedom	10	19	19	12	12	12	12
R square	0.9404	0.9846	0.9804	0.9191	0.8833	0.9647	0.9933
Absolute Sum of Squares	56423	2276	81.23	8893	192.4	1562	1205
Sy.x	75.12	10.95	2.068	27.22	4.004	11.41	10.02
Constraints							
K_m	Km > 0,0	Km > 0.0	Km > 0.0	Km > 0.0	Km > 0.0	Km > 0.0	Km > 0.0
Number of points							
Analyzed	12	21	21	14	14	14	14

GraphPad Prism 5.03	A16_Spd E1	A16_Spd E2	A13_Spd E1	A13_Spd E2	A12_Spd E1	A12_Spd E2	A18_Spd E1	A18_Spd E2
	nmol/min/mg	nmol/min/mg	nmol/min/mg	nmol/min/mg	nmol/min/mg	nmol/min/mg	nmol/min/mg	nmol/min/mg
Michaelis-Menten	E2			E1	E2	E1	E2	
Best-fit values								
V_{max}	112.9	26.35	7527	198.6	5562	489.6	495.2	492.9
K_m	1.317	41.54	138.9	46.79	138.0	95.59	25.38	54.86
Std. Error								
V_{max}	1.894	1.490	171.8	9.048	105.8	11.4	10.63	10.19
K_m	0.9901	9.555	9.217	6.131	7.645	7.065	2.419	3.630
95% Confidence Intervals								
V_{max}	108.8 to 117.0	23.10 to 29.60	7167 to 7887	179.1 to 218.2	5341 to 5783	465.8 to 513.5	472.7 to 517.8	471.3 to 514.5
K_m	0.0 to 3.475	20.72 to 62.36	119.6 to 158.1	33.55 to 60.03	122.0 to 154.0	80.80 to 110.4	20.25 to 30.51	47.16 to 62.55
Goodness of Fit								
Degrees of Freedom	12	12	19	13	19	19	16	16
R square	0.1380	0.7713	0.9860	0.9309	0.9899	0.9772	0.9374	0.9797
Absolute Sum of Squares	285.7	86.03	1.120e+006	1075	427845	6996	6620	3649
Sy.x	4.879	2.677	242.8	9.094	150.1	19.19	20.34	15.10
Constraints								
K_m	Km > 0.0	Km > 0.0	Km > 0.0	Km > 0.0	Km > 0.0	Km > 0.0	Km > 0.0	Km > 0.0
Number of points								
Analyzed	14	14	21	15	21	21	18	18

GraphPad Prism 5.03	PL_Spd E1	A4_Spd E1	A4_Spd E2	A3_Spd E1	A3_Spd E2	A7_Spd E1	A7_Spd E2	A11_Spd E1	A11_Spd E2
	nmol/min/mg	nmol/min/mg	nmol/min/mg	nmol/min/mg	nmol/min/mg	nmol/min/mg	nmol/min/mg	nmol/min/mg	nmol/min/mg
Michaelis-Menten					E1	E2	E1	E2	
Best-fit values									
V_{max}	1148	136.3	226.3	1422	438.5	1062	29.53	380.9	52.45
K_m	32.75	~ 1.284e-016	216.6	184.7	295.7	16.08	~ 1.883e-016	5.338	4.719
Std. Error									
V_{max}	29.82	4.365	3.984	44.78	9.985	41.33	1.964	5.627	0.8756
K_m	3.352		9.974	15.82	16.23	3.137		0.8642	0.8453
95% Confidence Intervals									
V_{max}	1084 to 1211	127.2 to 145.5	218.0 to 234.7	1328 to 1515	417.6 to 459.4	972.5 to 1151	25.16 to 33.91	368.7 to 393.0	50.50 to 54.40
K_m	25.65 to 39.86		195.8 to 237.5	151.6 to 217.8	261.7 to 329.7	9.307 to 22.86		3.471 to 7.205	2.836 to 6.603
Goodness of Fit									
Degrees of Freedom	16	19	19	19	19	13	10	13	10
R square	0.9349	-4,441e-016	0.9946	0.9780	0.9940	0.8107	-4.441e-016	0.7998	0.8047
Absolute Sum of Squares	44961	3746	349.7	54639	1370	54501	110.0	1586	15.59
Sy.x	53.01	14.04	4.290	53.63	8.491	64.75	3.317	11.04	1.249
Constraints									
K_m	Km > 0.0	Km > 0.0	Km > 0.0	Km > 0.0	Km > 0.0	Km > 0.0	Km > 0.0	Km > 0.0	Km > 0.0
Number of points									
Analyzed	18	21	21	21	21	15	12	15	12

Inhibition of SMO by covalently modified (*R*)-MeSpd (*S*)-MeSpd derivatives

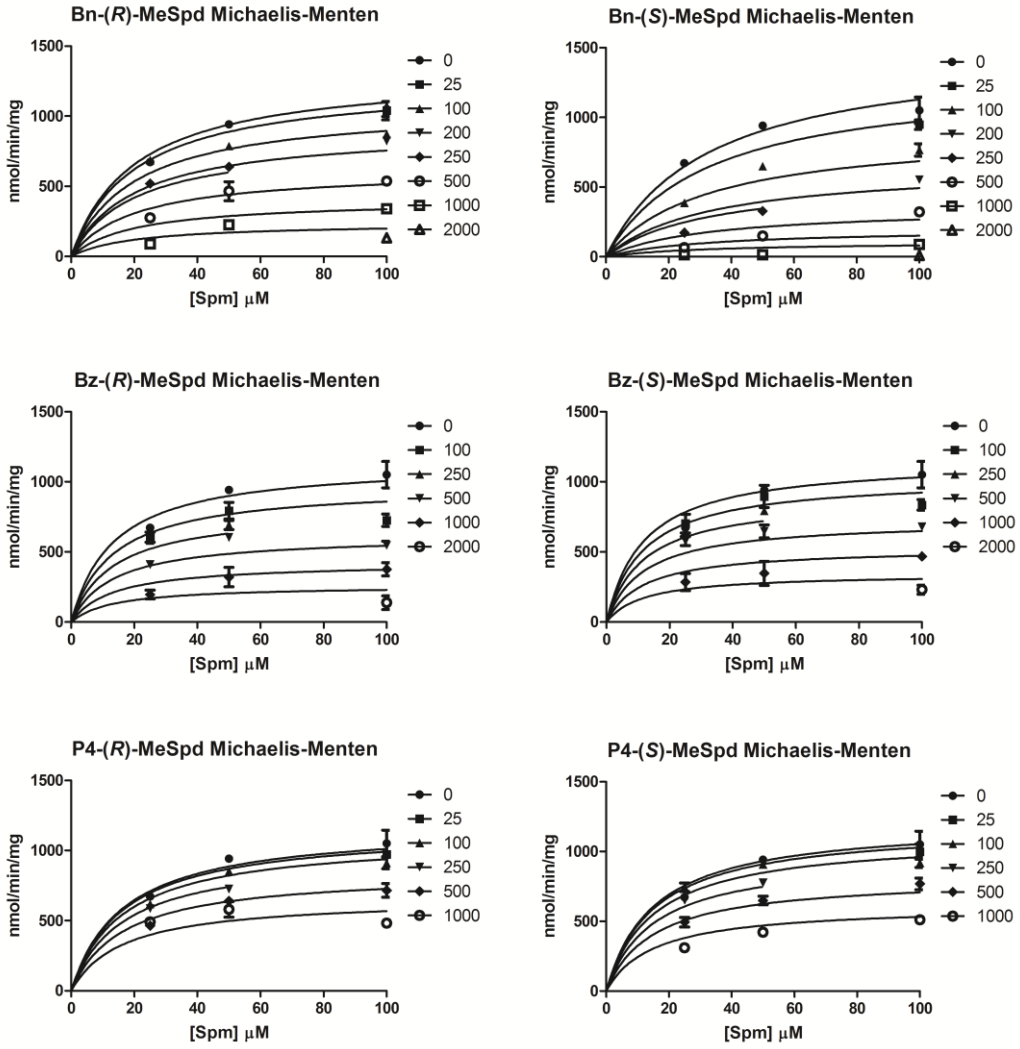

GraphPad Prism 5.03	Global (shared)	Global (shared)	Global (shared)	Global (shared)	Global (shared)	Global (shared)
Noncompetitive inhibition	Bn-(*R*)-MeSpd	Bn-(*S*)-MeSpd	Bz-(*R*)-MeSpd	Bz-(*S*)-MeSpd	P4-(*R*)-MeSpd	P4-(*S*)-MeSpd
Best-fit values						
V_{max}	1320	1502	1141	1154	1178	1215
I						
K_i	440.8	155	589	846	1277	1016
K_m	20.26	32.94	13.41	11.79	16.45	15.21
Std. Error						
V_{max}	50.8	89.27	57.86	53.07	36.78	36.77
K_i	32.26	12.61	56.77	81.95	110.7	79.12
K_m	2.792	5.471	2.831	2.422	2.009	1.900
95% Confidence Intervals						
V_{max}	1218 to 1422	1322 to 1681	1024 to 1258	1047 to 1261	1104 to 1252	1140 to 1289
K_i	375.9 to 505.7	129.6 to 180.3	474.4 to 703.6	680.6 to 1011	1054 to 1500	856.4 to 1176
K_m	14.65 to 25.88	21.93 to 43.95	7.695 to 19.13	6.904 to 16.68	12.40 to 20.51	11.38 to 19.05
Goodness of Fit						
Degrees of Freedom	48	48	42	42	42	42
R square	0.9526	0.9594	0.907	0.893	0.9071	0.9299
Absolute Sum of Squares	216629	255707	264780	267496	144692	146945
Sy.x	67.18	72.99	79.4	79.81	58.69	59.15

Bn-(*R*)-MeSpd

Nonlin fit	A	B	C	D	E	F	G	H	I
	0	25	100	200	250	500	1000	2000	Global (shared)
	Y	Y	Y	Y	Y	Y	Y	Y	Y
Noncompetitive inhibition									
Best-fit values									
Vmax	1320	1320	1320	1320	1320	1320	1320	1320	1320
I	= 0.0	= 25.00	= 100.0	= 200.0	= 250.0	= 500.0	= 1000	= 2000	
Ki	440.8	440.8	440.8	440.8	440.8	440.8	440.8	440.8	440.8
KM	20.26	20.26	20.26	20.26	20.26	20.26	20.26	20.26	20.26
Std. Error									
Vmax	50.80	50.80	50.80	50.80	50.80	50.80	50.80	50.80	50.80
Ki	32.26	32.26	32.26	32.26	32.26	32.26	32.26	32.26	32.26
KM	2.792	2.792	2.792	2.792	2.792	2.792	2.792	2.792	2.792
95% Confidence Intervals									
Vmax	1218 to 1422	1218 to 1422	1218 to 1422	1218 to 1422	1218 to 1422	1218 to 1422	1218 to 1422	1218 to 1422	1218 to 1422
Ki	375.9 to 505.7	375.9 to 505.7	375.9 to 505.7	375.9 to 505.7	375.9 to 505.7	375.9 to 505.7	375.9 to 505.7	375.9 to 505.7	375.9 to 505.7
KM	14.65 to 25.88	14.65 to 25.88	14.65 to 25.88	14.65 to 25.88	14.65 to 25.88	14.65 to 25.88	14.65 to 25.88	14.65 to 25.88	14.65 to 25.88
Goodness of Fit									
Degrees of Freedom									48
R square	0.8583	-0.0001727	0.4070	-2020	0.3498	0.7719	0.3007	-11.20	0.9526
Absolute Sum of Squares	34954	8473	33931	13719	15526	27868	67744	14415	216629
Sy.x									67.18
Constraints									
Vmax	Vmax is shared	Vmax is shared	Vmax is shared	Vmax is shared	Vmax is shared	Vmax is shared	Vmax is shared	Vmax is shared	
I	I = 0.0	I = 25.00	I = 100.0	I = 200.0	I = 250.0	I = 500.0	I = 1000	I = 2000	
Ki	Ki is shared	Ki is shared	Ki is shared	Ki is shared	Ki is shared	Ki is shared	Ki is shared	Ki is shared	
KM	KM is shared	KM is shared	KM is shared	KM is shared	KM is shared	KM is shared	KM is shared	KM is shared	
Number of points									
Analyzed	9	3	9	3	6	9	9	3	

Bn-(*S*)-MeSpd

Nonlin fit	A	B	C	D	E	F	G	H	I
	0	25	100	200	250	500	1000	2000	Global (shared)
	Y	Y	Y	Y	Y	Y	Y	Y	Y
Noncompetitive inhibition									
Best-fit values									
Vmax	1502	1502	1502	1502	1502	1502	1502	1502	1502
I	= 0.0	= 25.00	= 100.0	= 200.0	= 250.0	= 500.0	= 1000	= 2000	
Ki	155.0	155.0	155.0	155.0	155.0	155.0	155.0	155.0	155.0
KM	32.94	32.94	32.94	32.94	32.94	32.94	32.94	32.94	32.94
Std. Error									
Vmax	89.27	89.27	89.27	89.27	89.27	89.27	89.27	89.27	89.27
Ki	12.61	12.61	12.61	12.61	12.61	12.61	12.61	12.61	12.61
KM	5.471	5.471	5.471	5.471	5.471	5.471	5.471	5.471	5.471
95% Confidence Intervals									
Vmax	1322 to 1681	1322 to 1681	1322 to 1681	1322 to 1681	1322 to 1681	1322 to 1681	1322 to 1681	1322 to 1681	1322 to 1681
Ki	129.6 to 180.3	129.6 to 180.3	129.6 to 180.3	129.6 to 180.3	129.6 to 180.3	129.6 to 180.3	129.6 to 180.3	129.6 to 180.3	129.6 to 180.3
KM	21.93 to 43.95	21.93 to 43.95	21.93 to 43.95	21.93 to 43.95	21.93 to 43.95	21.93 to 43.95	21.93 to 43.95	21.93 to 43.95	21.93 to 43.95
Goodness of Fit									
Degrees of Freedom									48
R square	0.8261	-0.8254	0.7670	-24.79	0.5074	0.5576	-4.464	-34.94	0.9594
Absolute Sum of Squares	42894	4079	54084	11245	17851	45885	63940	15729	255707
Sy.x									72.99
Constraints									
Vmax	Vmax is shared	Vmax is shared	Vmax is shared	Vmax is shared	Vmax is shared	Vmax is shared	Vmax is shared	Vmax is shared	
I	I = 0.0	I = 25.00	I = 100.0	I = 200.0	I = 250.0	I = 500.0	I = 1000	I = 2000	
Ki	Ki is shared	Ki is shared	Ki is shared	Ki is shared	Ki is shared	Ki is shared	Ki is shared	Ki is shared	
KM	KM is shared	KM is shared	KM is shared	KM is shared	KM is shared	KM is shared	KM is shared	KM is shared	
Number of points									
Analyzed	9	3	9	3	6	9	9	3	

Bz-(*R*)-MeSpd

Nonlin fit	A	B	C	D	E	F	G
	0	100	250	500	1000	2000	Global (shared)
	Y	Y	Y	Y	Y	Y	Y
Noncompetitive inhibition							
Best-fit values							
Vmax	1141	1141	1141	1141	1141	1141	1141
I	= 0.0	= 100.0	= 250.0	= 500.0	= 1000	= 2000	
Ki	589.0	589.0	589.0	589.0	589.0	589.0	589.0
KM	13.41	13.41	13.41	13.41	13.41	13.41	13.41
Std. Error							
Vmax	57.86	57.86	57.86	57.86	57.86	57.86	57.86
Ki	56.77	56.77	56.77	56.77	56.77	56.77	56.77
KM	2.831	2.831	2.831	2.831	2.831	2.831	2.831
95% Confidence Intervals							
Vmax	1024 to 1258	1024 to 1258	1024 to 1258	1024 to 1258	1024 to 1258	1024 to 1258	1024 to 1258
Ki	474.4 to 703.6	474.4 to 703.6	474.4 to 703.6	474.4 to 703.6	474.4 to 703.6	474.4 to 703.6	474.4 to 703.6
KM	7.695 to 19.13	7.695 to 19.13	7.695 to 19.13	7.695 to 19.13	7.695 to 19.13	7.695 to 19.13	7.695 to 19.13
Goodness of Fit							
Degrees of Freedom							42
R square	0.8183	-0.04134	-0.09510	0.2597	0.4697	-5.174	0.9070
Absolute Sum of Squares	44813	71881	28650	54106	35553	29777	264780
Sy.x							79.40
Constraints							
Vmax	Vmax is shared	Vmax is shared	Vmax is shared	Vmax is shared	Vmax is shared	Vmax is shared	
I	I = 0.0	I = 100.0	I = 250.0	I = 500.0	I = 1000	I = 2000	
Ki	Ki is shared	Ki is shared	Ki is shared	Ki is shared	Ki is shared	Ki is shared	
KM	KM is shared	KM is shared	KM is shared	KM is shared	KM is shared	KM is shared	
Number of points							
Analyzed	9	9	6	9	9	3	

Bz-(*S*)-MeSpd

Nonlin fit	A	B	C	D	E	F	G
	0	100	250	500	1000	2000	Global (shared)
	Y	Y	Y	Y	Y	Y	Y
Noncompetitive inhibition							
Best-fit values							
Vmax	1154	1154	1154	1154	1154	1154	1154
I	= 0.0	= 100.0	= 250.0	= 500.0	= 1000	= 2000	
Ki	846.0	846.0	846.0	846.0	846.0	846.0	846.0
KM	11.79	11.79	11.79	11.79	11.79	11.79	11.79
Std. Error							
Vmax	53.07	53.07	53.07	53.07	53.07	53.07	53.07
Ki	81.95	81.95	81.95	81.95	81.95	81.95	81.95
KM	2.422	2.422	2.422	2.422	2.422	2.422	2.422
95% Confidence Intervals							
Vmax	1047 to 1261	1047 to 1261	1047 to 1261	1047 to 1261	1047 to 1261	1047 to 1261	1047 to 1261
Ki	680.6 to 1011	680.6 to 1011	680.6 to 1011	680.6 to 1011	680.6 to 1011	680.6 to 1011	680.6 to 1011
KM	6.904 to 16.68	6.904 to 16.68	6.904 to 16.68	6.904 to 16.68	6.904 to 16.68	6.904 to 16.68	6.904 to 16.68
Goodness of Fit							
Degrees of Freedom							42
R square	0.7674	0.2974	0.2307	-0.8618	0.2090	-8.157	0.8930
Absolute Sum of Squares	57371	58628	30219	42190	59332	19757	267496
Sy.x							79.81
Constraints							
Vmax	Vmax is shared	Vmax is shared	Vmax is shared	Vmax is shared	Vmax is shared	Vmax is shared	
I	I = 0.0	I = 100.0	I = 250.0	I = 500.0	I = 1000	I = 2000	
Ki	Ki is shared	Ki is shared	Ki is shared	Ki is shared	Ki is shared	Ki is shared	
KM	KM is shared	KM is shared	KM is shared	KM is shared	KM is shared	KM is shared	
Number of points							
Analyzed	9	9	6	9	9	3	

P4-(*R*)-MeSpd

Nonlin fit	A	B	C	D	E	F	G
	0	25	100	250	500	1000	Global (shared)
	Y	Y	Y	Y	Y	Y	Y
1 Noncompetitive inhibition							
2 Best-fit values							
3 Vmax	1178	1178	1178	1178	1178	1178	1178
4 I	= 0.0	= 25.00	= 100.0	= 250.0	= 500.0	= 1000	
5 Ki	1277	1277	1277	1277	1277	1277	1277
6 KM	16.45	16.45	16.45	16.45	16.45	16.45	16.45
7 Std. Error							
8 Vmax	36.78	36.78	36.78	36.78	36.78	36.78	36.78
9 Ki	110.7	110.7	110.7	110.7	110.7	110.7	110.7
10 KM	2.009	2.009	2.009	2.009	2.009	2.009	2.009
11 95% Confidence Intervals							
12 Vmax	1104 to 1252	1104 to 1252	1104 to 1252	1104 to 1252	1104 to 1252	1104 to 1252	1104 to 1252
13 Ki	1054 to 1500	1054 to 1500	1054 to 1500	1054 to 1500	1054 to 1500	1054 to 1500	1054 to 1500
14 KM	12.40 to 20.51	12.40 to 20.51	12.40 to 20.51	12.40 to 20.51	12.40 to 20.51	12.40 to 20.51	12.40 to 20.51
15 Goodness of Fit							
16 Degrees of Freedom							42
17 R square	0.8510	-2.724	0.9022	0.9217	0.8771	-1.985	0.9071
18 Absolute Sum of Squares	36753	1510	14388	2362	13046	76633	144692
19 Sy.x							58.69
20 Constraints							
21 Vmax	Vmax is shared	Vmax is shared	Vmax is shared	Vmax is shared	Vmax is shared	Vmax is shared	
22 I	I = 0.0	I = 25.00	I = 100.0	I = 250.0	I = 500.0	I = 1000	
23 Ki	Ki is shared	Ki is shared	Ki is shared	Ki is shared	Ki is shared	Ki is shared	
24 KM	KM is shared	KM is shared	KM is shared	KM is shared	KM is shared	KM is shared	
25 Number of points							
26 Analyzed	9	3	9	6	9	9	
27							

P4-(*S*)-MeSpd

Nonlin fit	A	B	C	D	E	F	G
	0	25	100	250	500	1000	Global (shared)
	Y	Y	Y	Y	Y	Y	Y
1 Noncompetitive inhibition							
2 Best-fit values							
3 Vmax	1215	1215	1215	1215	1215	1215	1215
4 I	= 0.0	= 25.00	= 100.0	= 250.0	= 500.0	= 1000	
5 Ki	1016	1016	1016	1016	1016	1016	1016
6 KM	15.21	15.21	15.21	15.21	15.21	15.21	15.21
7 Std. Error							
8 Vmax	36.77	36.77	36.77	36.77	36.77	36.77	36.77
9 Ki	79.12	79.12	79.12	79.12	79.12	79.12	79.12
10 KM	1.900	1.900	1.900	1.900	1.900	1.900	1.900
11 95% Confidence Intervals							
12 Vmax	1140 to 1289	1140 to 1289	1140 to 1289	1140 to 1289	1140 to 1289	1140 to 1289	1140 to 1289
13 Ki	856.4 to 1176	856.4 to 1176	856.4 to 1176	856.4 to 1176	856.4 to 1176	856.4 to 1176	856.4 to 1176
14 KM	11.38 to 19.05	11.38 to 19.05	11.38 to 19.05	11.38 to 19.05	11.38 to 19.05	11.38 to 19.05	11.38 to 19.05
15 Goodness of Fit							
16 Degrees of Freedom							42
17 R square	0.8394	-0.4236	0.4561	0.5112	0.8237	0.5858	0.9299
18 Absolute Sum of Squares	39617	8747	36964	14122	21386	26109	146945
19 Sy.x							59.15
20 Constraints							
21 Vmax	Vmax is shared	Vmax is shared	Vmax is shared	Vmax is shared	Vmax is shared	Vmax is shared	
22 I	I = 0.0	I = 25.00	I = 100.0	I = 250.0	I = 500.0	I = 1000	
23 Ki	Ki is shared	Ki is shared	Ki is shared	Ki is shared	Ki is shared	Ki is shared	
24 KM	KM is shared	KM is shared	KM is shared	KM is shared	KM is shared	KM is shared	
25 Number of points							
26 Analyzed	9	3	9	6	9	9	
27							
28							

Michaelis-Menten Graphs and Data of **Supplementary Material 1** Tables 1 and 2

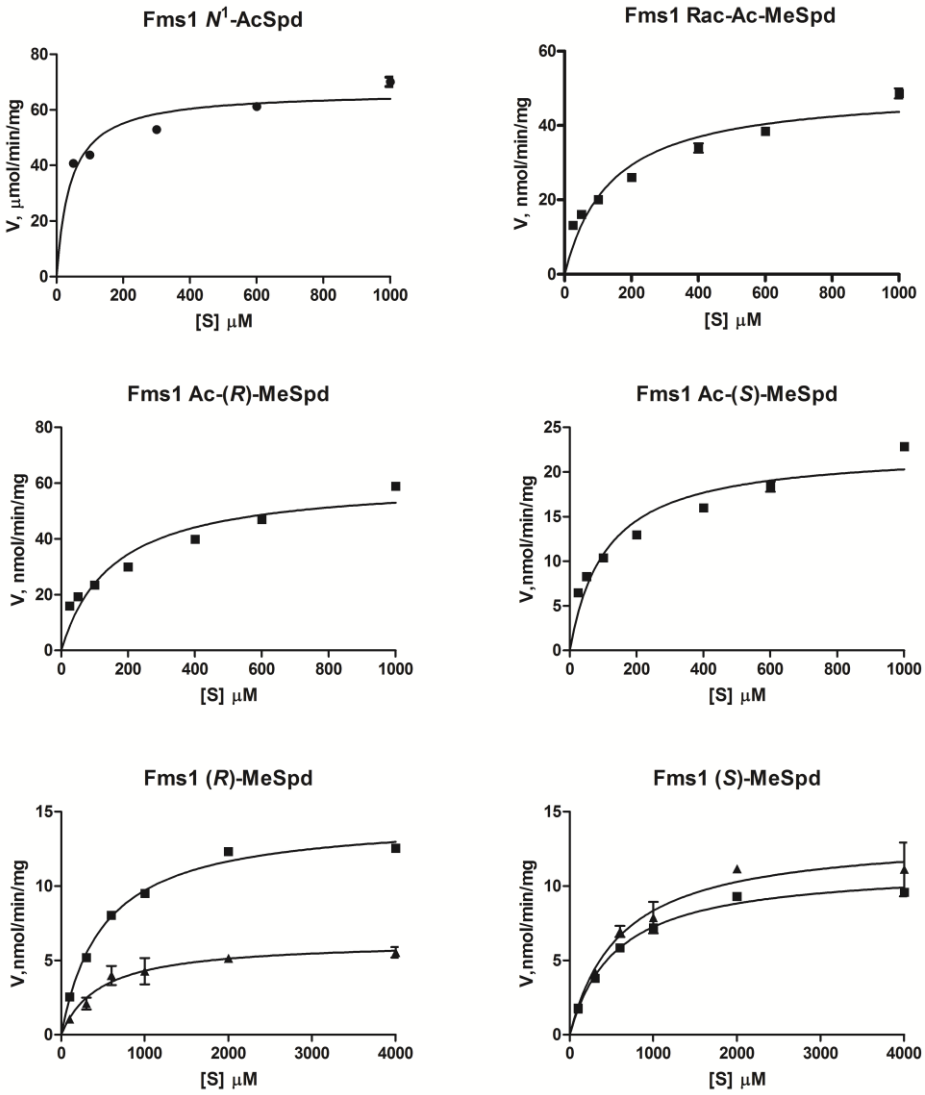

GraphPad Prism 5.03	N^1AcSpd	Rac-AcMeSpd	Ac-(*R*)-MeSpd	Ac-(*S*)-MeSpd	(*R*)-MeSpd	(*R*)-MeSpd	(*S*)-MeSpd	(*S*)-MeSpd
	μmol/min/mg	nmol/min/mg	nmol/min/mg	nmol/min/mg	nmol/min/mg	nmol/min/mg	nmol/min/mg	nmol/min/mg
Michaelis-Menten					E1	E2	E1	E2
Best-fit values								
V_{max}	66.65	49.78	61.24	22.51	14.59	6.315	11.28	13.40
K_m	41.78	139.3	154.8	109.2	502.2	466.6	555.1	606.0
Std. Error								
V_{max}	2.294	2.568	3.584	1.054	0.2778	0.3535	0.2146	0.7203
K_m	7.564	23.43	28.59	17.97	31.11	87.16	33.19	99.42
95% Confidence Intervals								
V_{max}	61.69 to 71.60	44.41 to 55.15	53.74 to 68.74	20.31 to 24.72	14.00 to 15.18	5.565 to 7.064	10.83 to 11.74	11.87 to 14.92
K_m	25.44 to 58.12	90.22 to 188.3	94.97 to 214.6	71.63 to 146.8	436.2 to 568.1	281.8 to 651.4	484.7 to 625.4	395.3 to 816.8
Goodness of Fit								
Degrees of Freedom	13	19	19	19	16	16	16	16
R square	0.8226	0.9099	0.8962	0.9027	0.9898	0.9156	0.9909	0.9396
Absolute Sum of Squares	316.5	271.1	464.4	59.74	2.402	4.183	1.292	13.25
Sy.x	4.934	3.778	4.944	1.773	0.3874	0.5113	0.2842	0.9099
Constraints								
K_m	Km > 0.0	Km > 0.0	Km > 0.0	Km > 0.0	Km > 0.0	Km > 0.0	Km > 0.0	Km > 0.0
Number of points								
Analyzed	15	21	21	21	18	18	18	18